Molecular Simulation of Nonfacillitated Membrane Permeation

Ernest Awoonor-Williams, Christopher N. Rowley

Department of Chemistry, Memorial University of Newfoundland, St. John's, NL A1B 3X7 Canada

---

Abstract

A review with 175 references. Non-electrolytic compounds typically cross cell membranes by passive diffusion. The rate of permeation is dependent on the chemical properties of the solute and the composition of the lipid bilayer membrane. Predicting the permeability coefficient of a solute is important in pharmaceutical chemistry and toxicology. Molecular simulation has proven to be a valuable tool for modeling permeation of solutes through a lipid bilayer. In particular, the solubility-diffusion model has allowed for the quantitative calculation of permeability coefficients. The underlying theory and computational methods used to calculate membrane permeability are reviewed. We also discuss applications of these methods to examine the permeability of solutes and the effect of membrane composition on permeability. The application of coarse grain and polarizable models is discussed.

Keywords: review, membrane, lipid bilayer, permeation, non-facilitated, solubility-diffusion model, molecular dynamics, diffusion, PMF, potential of mean force, polarizable, coarse grained

---

Preprint submitted to BBA - Biomembranes *October 13, 2015*

1. Introduction

One function of a biological membranes is to serve as a barrier between the cytosol and extracellular environment (1; 2; 3). Intracellular compartments like mitochondria, the nucleus, etc, are also enclosed by membranes. The primary component of these membranes are amphiphilic lipids. These lipids consist of a polar or ionic headgroup and a tail that is comprised of one or more hydrocarbon chain. The hydrophilicity of the head groups and the hydrophobicity of the tails causes the lipids to spontaneously self-assemble into planar bilayers where the headgroups face the solution and the tails form a hydrophobic interior layer.

Solutes crossing the membrane must pass through the non-polar lipid tail region of the membrane. Compounds that are more soluble in bulk water than they are in the non-polar membrane interior will tend not to partition into the membrane. This simple mechanism allows these thin bilayers ($\sim 40-50$ Å thick) to provide an effective barrier for highly water-soluble compounds like ions and sugars. In pure lipid bilayers, the rates of permeation of these species are very low. In biological membranes, rapid permeation of these compounds can be facilitated by membrane proteins like channels or transporters (4; 5; 6).

Two distinct mechanisms have been proposed for permeation in the absence of a protein facilitator: passage through a transient water pore and direct permeation through the membrane (7). Rare fluctuations in the bilayer can form transient water pores that allow ionic compounds to cross the bilayer while still solvated by water. This avoids the high thermodynamic penalty for dehydrating the ion. The second mechanism applies to non-electrolytic solutes, which can permeate directly through the membrane. This review will focus on molecular simulations of this second mechanism.

Many non-electrolytic compounds can permeate directly through the membrane because there is a significant probability for them to partition into the interior of the membrane. These compounds are generally only moderately soluble in aqueous solutions due to the lack of strong electrostatic interactions with water molecules. The London dispersion attractions between these solutes and the lipid tails can be competitive to their interactions with water, so the thermodynamic penalty for these compounds to enter the interior of the membrane is attenuated or even eliminated. To varying degrees, these compounds can undergo direct permeation without facilitation by a transmembrane protein.

The rate of permeation of a solute across a membrane is defined by its flux (J), which gives the number of molecules that cross a unit area of the membrane per unit time (e.g., μmol/s/cm^2). The flux is the product of the concentration gradient of the solute across the membrane (ΔC) and the permeability coefficient (P),

$$J = P \cdot \Delta C. \tag{1}$$

P depends on the type of permeating solute, the membrane composition, and the conditions of permeation occurs under (e.g., temperature). It has units of distance per unit time and is commonly reported in cm/s. Under common conditions and membrane composition, the permeability coefficient provides a measure of the intrinsic membrane permeability of solutes. P is therefore the standard experimental and computational measure of the permeability of a solute.

Understanding the relationship between the chemical properties of the solute and its permeability is important for predicting the toxicity and pharmacokinetics of a compound (8; 9; 10). Publications by Meyer in 1899 and Overton in 1901 established the relationship between high rates of nonfacilitated membrane permeation and the hydrophobicity of the solute (11; 12). Walter and Gutknecht quantified this observation by showing that there is strong linear correlation between the log of the permeability coefficient and the log of water-alkane partition coefficients for a wide range of neutral solutes (13). This supports the Meyer–Overton rule that the rate of permeation is proportional to the relative solubility of the solute in the apolar membrane interior vs an aqueous solution.

Several experimental and theoretical models have been developed to predict permeability (14; 15; 16; 8; 9), with varying degrees of success, but the advent of computer simulations have led to the most significant developments. Molecular simulation methods for lipid bilayers have made it possible to study the permeation of solutes without direct empirical inputs. These simulations have provided atomic-scale interpretations of these data and quantitative interpretations of permeability trends in terms of the solution thermodynamics and dynamics. Empirically-based principles of permeation like the Meyer–Overton rule can now be interpreted within a rigorous physical framework. This review presents some of the research on the simulation of nonfacilitated permeation over the last 20 years. Interested readers may also be interested in a recent review by MacCallum and Tieleman on simulations of small molecules interacting with lipid bilayers (17) and a review by Orsi and Essex on modeling permeability (18).

2. Development of the Solubility-Diffusion Model

To develop a quantitative theory for nonfacillitated permeation, the membrane is described as a fluid environment that the permeant passes through by Brownian motion. This model is consistent with direct molecular dynamics simulations of membrane permeation. Figure 1 shows the trajectory of a O_2 molecule permeating through a DPPC bilayer. The solute undergoes an effectively random walk along the z-axis before exiting the opposite side of the membrane. The solute also undergoes significant lateral motion inside bilayer in the xy plane, but a rate theory can be developed based on the net flux (J) of the solute along the z-axis alone.

The dynamics of the solute are complicated by the inhomogeneity of the bilayer, which varies in chemical composition and density along the transmembrane axis, z. In this model, both the solute diffusivity ($D(z)$) and potential of mean force (PMF, $w(z)$) vary as a function of the position of the solute along the z axes. $w(z)$ is related to the solubility of the solute at z, $K(z) = \exp(-w(z)/k_BT)$, so this model is commonly referred to as the solubility-diffusion model.

The one-dimensional Nernst–Planck equation for a neutral solute in an inhomogeneous medium (19; 20) provides an expression for the flux through a unit area of the membrane depth z ($J(z)$),

$$J(z) = -D(z)\frac{\mathrm{d}C(z)}{\mathrm{d}z} - C(z)D(z)\frac{\mathrm{d}\left(w(z)/k_BT\right)}{\mathrm{d}z}, \tag{2}$$

where $C(z)$ is the concentration of the solute.

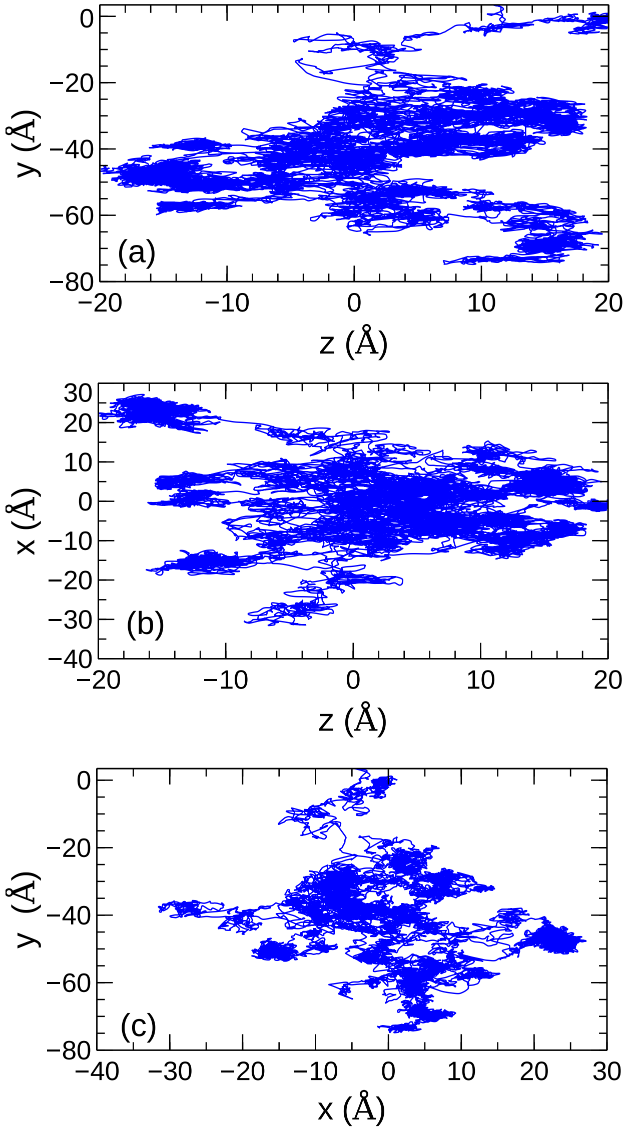

Figure 1: 2D representations of a 300 ps trajectory of an O_2 molecule permeating from the lower interface ($z = -20$ Å) to the upper interface ($z = 20$ Å) of a DPPC bilayer. The z axis corresponds to permeation across the bilayer, while the x and y axes are in the plane of the bilayer–water interface. The trajectory plotted in (a) and (b) show permeation consistent with Brownian motion, with the solute moving back and forth along the z axis before reaching the opposite interface ($z = 20$ Å). Plot (c) shows that there is significant lateral diffusion of the solute in the xy-plane during permeation.

Multiplying both sides of the equation by $e^{w(z)/k_BT}/D(z)$ gives,

$$\frac{J(z)e^{w(z)/k_BT}}{D(z)} = -e^{w(z)/k_BT}\frac{\mathrm{d}C(z)}{\mathrm{d}z} - e^{w(z)/k_BT}C(z)\frac{\mathrm{d}\left(w(z)/k_BT\right)}{\mathrm{d}z} \tag{3}$$

The right hand side of this equation can be combined into a single differential,

$$\frac{J(z)e^{w(z)/k_BT}}{D(z)} = -\frac{\mathrm{d}}{\mathrm{d}z}\left(C(z)e^{w(z)/k_BT}\right) \tag{4}$$

To determine the flux across the entire bilayer, this equation is integrated with respect to z over the interval $[-L/2, L/2]$ where L is the width of a bilayer centered at $z = 0$,

$$\int_{-L/2}^{L/2}\frac{J(z)e^{w(z)/k_BT}}{D(z)}\mathrm{d}z = -\int_{-L/2}^{L/2}\frac{\mathrm{d}}{\mathrm{d}z}\left(C(z)e^{w(z)/k_BT}\right)\mathrm{d}z \tag{5}$$

Under steady-state conditions, the flux at any value of z will be constant, so J can be factored out of the integral. Through rearrangement and simplification, the equation becomes,

$$J\int_{-L/2}^{L/2}\frac{e^{w(z)/k_BT}}{D(z)}\mathrm{d}z = -\left[C(z)e^{w(z)/k_BT}\right]_{-L/2}^{L/2} \tag{6}$$

Isolating J on the left hand side and evaluating the bounds on the integral on the right hand side gives,

$$J = -\frac{1}{\int_{-L/2}^{L/2}\frac{e^{w(z)/k_BT}}{D(z)}\mathrm{d}z}\left[C(L/2)e^{w(L/2)/k_BT} - C(-L/2)e^{w(-L/2)/k_BT}\right] \tag{7}$$

By definition, $w(z)$ is zero in the solution outside the bilayer, so $w(L/2) = w(-L/2) = 0$. This gives the final form of the equation for the flux,

$$J = -\frac{1}{\int_{-L/2}^{L/2}\frac{e^{w(z)/k_BT}}{D(z)}\mathrm{d}z}\left[C(L/2) - C(-L/2)\right]. \tag{8}$$

$C(-L/2) - C(L/2)$ is the concentration difference across the bilayer in the direction of the positive flux, ΔC. By comparison to Eqn. 1, the permeability coefficient is,

$$\frac{1}{P} = \int_{-L/2}^{L/2} \frac{e^{w(z)/k_B T}}{D(z)} \mathrm{d}z \tag{9}$$

Alternative derivations are available in Diamond and Katz (21) and Marrink and Berendsen (22; 23). An elaboration that includes the orientational degrees of freedom of the solute is presented in Ref. 24.

Several assumptions are made in this derivation. The flux is assumed to be under steady state conditions with a negligible concentration gradient across the membrane. The membrane must be sufficiently laterally homogeneous so that meaningful averages of $w(z)$ and $D(z)$ can be determined. For example, a permeability rate that is governed by the formation of a water-pore that allows passage of the solute would not be well described by this model (7; 25). The solute dynamics are described by Brownian motion, which is only valid for individual solute molecules moving through high-friction environments on a reasonably flat free energy surface. The permeation of a solute with a variable number of associated water molecules would also be affected by the rates of hydration/dehydration inside the membrane and is not entirely consistent with this model.

To calculate P using this theory, $D(z)$ and $w(z)$ must be determined for the full width of the membrane. These data can then be used to evaluate the integral in Eqn. 9 numerically. The practical aspects of calculating these profiles is presented in the following sections.

3. Practical Aspects

3.1. Simulation Systems

Simulations of membrane permeability are typically performed with periodic unit cells. A planar bilayer is constructed in the cell to form a lamellar system. Water layers are added above and below the bilayer. By convention, the bilayer interface extends along the xy plane and the z-axis corresponds to the transmembrane axis (a.k.a., the bilayer normal). Recent simulations comonly include 60–200 lipids (26; 27; 28). The water layers must be sufficiently thick so that periodic membrane–membrane interactions are minimized and so $D(z)$ and $w(z)$ can be calculated at distances that are sufficiently far from the water-lipid interface to establish a reference (i.e., $w(z_{\mathrm{bulk}}) = 0$). Studies have used simulation cells with various sizes, but bilayer surface areas in the $40 - 60$ Å range and $80 - 110$ Å in the z dimension are common. A typical simulation cell is shown in Figure 2.

A wide range of force fields have been used in recent permeation simulations. The TIP3P (29) and TIP4P (30) water models are both popular. The Berger (31) and CHARMM (32) lipid models have both been used successfully. The permeating solutes have been described using specific force fields or generalized force fields like GAFF (33), OPLS (34), or CGenFF (35). Polarizable and coarse grain models are also available. These are discussed in Sections 5.1 and 5.2.

3.2. Calculation of the Potential of Mean Force

The potential of mean force of the permeation of the solute along the z-axis ($w(z)$) can be calculated using a range of free energy methods. The

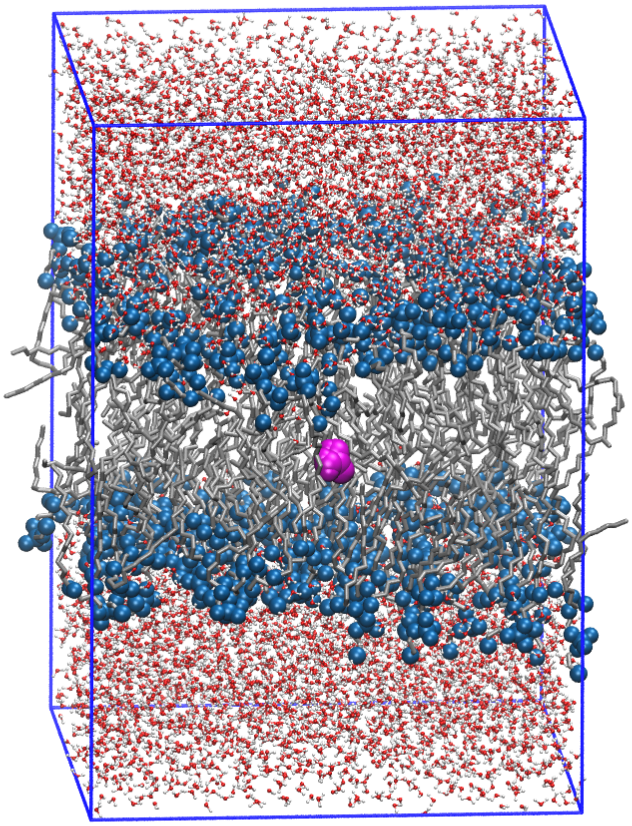

Figure 2: An example simulation cell used to simulate membrane permeation. A bilayer section with a 62 Å × 62 Å surface area and containing 128 1,2-dimyristoyl-sn-glycero-3-phosphocholine (DMPC) lipids is oriented in the *xy* plane of the cell. Lipid tails are rendered in gray and lipid heads are rendered in blue. The bilayer is surrounded by water layers (red and white). A permeating molecule of urea is at the center of the bilayer (magenta).

first PMFs calculated by Marrink and Berendsen used,

$$w(z) = -\int_{-L}^{z} \langle F_z(z') \rangle_{z'} \mathrm{d}z' \tag{10}$$

$F_z(z')$ is the force on the solute along the z-axis when the solute is contrained at z'.

To sample the ensemble average of $F_z(z')$, ($\langle F_z \rangle_{z'}$), the equations of motion must be modified so that the solute is constrained to a value of z'. The z-component of the force on the solute by the environment are averaged over long MD simulations at a series of positions spanning the membrane. The integral is numerically integrated to yield $w(z)$.

Most recent permeability simulations use umbrella sampling to calculate $w(z)$. In this method, a series simulations are performed with the solute restrained relative to the center of mass of the membrane using a harmonic potential,

$$u_i(z) = \frac{1}{2}k(z - z_{0,i})^2. \tag{11}$$

These simulations are performed at regular intervals across the membrane. The optimal choices of window spacing and force constant (k) depends on the membrane composition, temperature, and solute. Recent studies have used window spacings that vary between 0.25–1.0 Å separations and a force constants in the k=1.2–7.2 kJ mol^{-1} Å^{-2} range (36; 27; 37). In some systems, sections of the PMF may require more extensive sampling (38), so additional windows at smaller spacings and stronger force constants can be added in these regions (36).

Neale et al. showed that an umbrella sampling simulations for the partitioning of arginine and isoleucine side chain models into a bilayer required very extensive simulations to achieve sub-kcal convergence (38). This was particularly serious for the charged arginine group, which required a 125 ns equilibriation and μs length sampling per umbrella sampling window to eliminate systematic errors. This was attributed to distortions in the bilayer that occur over long timescales. Even the calculation of permeations PMFs of small non-polar solutes requires equilibriation simulations that are several nanoseconds long and a sampling period greater than 10 ns. Performing several independent simulations from different initial configurations can help identify if the PMF has reached convergence.

The slow convergence of permeation umbrella sampling simulations can be addressed by enhanced sampling techniques. Hamiltonian-exchange molecular dynamics allows neighboring windows of an umbrella sampling simulation to periodically exchange coordinates (39; 40). This can be applied to the calculation of membrane permeation PMFs by allowing exchanges of neighboring umbrella sampling windows along the z axis (e.g., $z_{0,4} = 4$ Å $\leftrightarrow z_{0,5} = 5$ Å$\leftrightarrow z_{0,6} = 6$ Å). Neale et al. (26) developed a Hamiltonian exchange method for membrane permeation PMFs based on the virtual replica exchange method of Rauscher et al. (41). This method was found to have 300% better sampling efficiency than conventional umbrella sampling simulations.

Huang and Garcia applied the Replica Exchange with Solute Tempering (REST) enhanced sampling method to the simulation of lipid bilayers (42). In this technique, the simulation of the bilayer is allowed to undergo exchanges with simulations where the lipid–lipid interactions solute and bilayer are coupled to different thermostats and lipid-lipid interactions are biased. This allows rapid lateral diffusion of the lipids and could improve the sampling of the configurational space of the permeating solutes.

The permeation of large amphiphilic solutes is complicated by the dynamics of secondary degrees of freedom. Even for small amphiphiles, like alcohols, the solute must undergo a “flip-flop” transition, where the hydrophilic head reorients to be directed towards the opposing membrane interface when it passes through the bilayer interior. Comer et al. developed a method that incorporates the dynamics of the solute along z and its orientation with respect to the xy plane of the membrane (43). Similarly, the Parisio et al. developed an extension to the solubility-diffusion model where the rotation of the solute is explicitly included (24).

3.3. Calculation of the Diffusivity Profile

The solubility-diffusion model requires the calculation of the diffusion coefficient of the solute as a function of the position of the solute along the z-axis ($D(z)$). The standard methods of calculating the diffusion coefficient of a solute from an MD simulation use the Einstein or Green–Kubo relations. These methods are not appropriate for calculating $D(z)$ because they assume the solution is homogenous, so they cannot capture the variation of D with the position of the solute along z.

Hummer developed a method to calculate position-dependent diffusion coefficients by sampling the frequency of transitions between positions along a coordinate in an equilibrium MD simulation (44). The variation of solubility of the solute in the bilayer is a challenge for this method. If the solubility of the solute is low at any point of the profile (i.e., $w(z)$ is large), transitions across this part of the profile in an equilibrium MD simulation will be rare.

Very extensive MD simulations would be needed to directly sample diffusion across the full bilayer except for the most permeable solutes.

One direct method of calculating $D(z)$ uses a relation from fluctuation–dissipation theory to calculate $D(z)$ using the autocorrelation function (ACF) of the force on the solute when it is constrained at position z along the axis (45),

$$D(z') = \frac{(RT)^2}{\int_0^\infty \langle \delta F_z(z',0)\delta F_z(z',t)\rangle \mathrm{d}t} \tag{12}$$

Here,$\delta F_z(z',t)$ is the deviation of the force on the solute along the z axis at position z' from the average force ($\delta F_z(z,t) = F_z(z,t) - \langle F_z(z')\rangle$).

In practice, these calculations make use of the same type of simulations that can be used to calculate the PMF from the integral of the average force (Eqn. 10). The drawback of this method is that most MD codes would have to be modified in order to do these calculations. The equations of motion of the MD integration algorithm must be modified to constrain the solute to a particular value of z (46). Most standard simulations codes must also be modified to output the time series of the force on a single molecule.

Alternative techniques for calculating $D(z)$ are provided by solutions to the Generalized Langevin Equation (GLE) for a harmonic oscillator. Consider a simulation where the permeant is restrained at some value of z along the transmembrane axis using a harmonic potential (i.e., Eqn. 11). The motion of the solute can be modeled as a harmonic oscillator where rest of the system serves at its frictional bath. The GLE expression for the dynamics of this oscillator is,

$$m\ddot{z} = -k(z - z_{0,i}) - m\int_0^t \dot{z}(\tau)M(t-\tau)\mathrm{d}\tau + R(t) \tag{13}$$

where $R(t)$ is the random force that originates from the degrees of freedom orthogonal to z. $M(t)$ is the memory kernel, which reflects the frictional forces on the solute. Beginning from this equation, Woolf and Roux derived an expression for the diffusion coefficient at $\langle z\rangle_i$ in terms of the Laplace transform of the velocity ACF ($\hat{C}(s;z_i)$) (47; 48; 49).

$$D(z_i = \langle z\rangle_i) = \lim_{s\to 0} \frac{-\hat{C}(s;z_i)\langle\delta z^2\rangle_i\langle\dot{z}^2\rangle_i}{\hat{C}(s;z_i)\left[s\langle\delta z^2\rangle_i + \langle\delta\dot{z}\rangle_i/s\right] - \langle\delta z^2\rangle_i\langle\dot{z}^2\rangle_i} \tag{14}$$

Because this equation has a singularity at $s = 0$, the limit cannot be taken directly. Instead, the Laplace transform must be performed numerically for a series of values of s and then the value of $s = 0$ must be extrapolated from these points.

Hummer derived a simpler expression based on this theory that relates $D(z)$ to the position ACF ($C_{zz}(t)$) (44).

$$D(z_i = \langle z\rangle_i) = \frac{\mathrm{var}(z)^2}{\int_0^\infty C_{zz}(t)\mathrm{d}t} \tag{15}$$

C_{zz} can be calculated by direct summation of pairs over the time series (50),

$$C_{zz}(t) = \langle\delta z(0)\delta z(t)\rangle = \frac{1}{n_{\mathrm{samples}}}\sum_{i=0}^{n_{\mathrm{samples}}} \delta z(i)\delta z(t+i) \tag{16}$$

where $\delta z(t) = z(t) - \langle z\rangle$.

A key advantage of these methods is that they only require that the solute be restrained at a point along z with a harmonic potential with a reference position relative to the center of mass of the bilayer. This type of restraint is simple to implement and are available in most molecular dynamics codes. The diffusivity profile of a solute can be calculated by performing a series of MD simulations where the solute is restrained to positions at regular intervals along the z axis (e.g., 1 Å apart). This procedure is directly analogous to the umbrella sampling simulations using harmonic restraints that are used to calculate $w(z)$. In principle, both properties could be calculated from the same simulations. A time-series of the z position of this solute is collected from each simulation, which are then used to calculate the ACF.

In practice, the calculation of $D(z)$ is highly sensitive to the equilibration of the system and the length of sampling. Multiple simulations that are several nanoseconds long are needed to calculate well-converged ACFs. The spring constants of the harmonic potential (k) can affect the results because the description of the system with the GLE is based on the system acting as a harmonic oscillator in a frictional bath. Deviations away from this harmonic-oscillator model due to the effect of a rough underlying free energy surface can introduce biases. Hummer also showed that $D(z)$ varies with the length of the interval the ACF is integrated over (44). Lastly, irregularities in the bilayer structure and the formation of water clusters around the solute can lead to large variations in $D(z)$. Improved methods for calculating position-dependent diffusivity profiles are an active subject of investigation (51; 52).

4. The Solubility-Diffusion Model in Practice

4.1. Interpreting Permeation Profiles

4.1.1. Bilayer Regions

The diffusion and PMF profiles calculated by Marrink and Berendsen illustrated how the bilayer environment varies with depth. The bilayer was divided into four overlapping regions that have different structural and chemical interactions with solutes, so the solutes will diffuse at different rates and have different solubility in these regions. The center of the bilayer is used as the point of reference ($z = 0$). The given ranges of z are approximate values for the DPPC bilayer example used in this review.

- Region I: $z > 25$ Å. The bulk solution. This region is primarily liquid water, with a small component of lipid headgroups.
- Region II: 17 Å $< z < 25$ Å. The lipid headgroups. These are typically solvated by water molecules.
- Region III: 10 Å $< z < 17$ Å. The upper portions of the lipid tails, acyl groups, and lower portions of the head groups.
- Region IV: $z < 10$ Å. The interface of the lipid tails of the two opposing monolayers at the center of the bilayer

These regions will be used to describe sections of the potential of mean force and diffusivity profiles discussed in the following sections. Marrink and Berendsen compared the PMFs of O_2 and H_2O as the prototypical examples of hydrophobic and hydrophilic permeants, respectively. These calculations were reproduced here using current models and simulation lengths (Figure 3).

4.1.2. Potential of Mean Force

The PMF, $w(z)$ (a.k.a., $\Delta G(z)$), is the reversible work needed to move the solute from solution to the position z on the transmembrane axis. The PMF corresponds to the relative solubility of the permeant in solution vs the membrane interior; a positive PMF indicates the solute is less soluble at

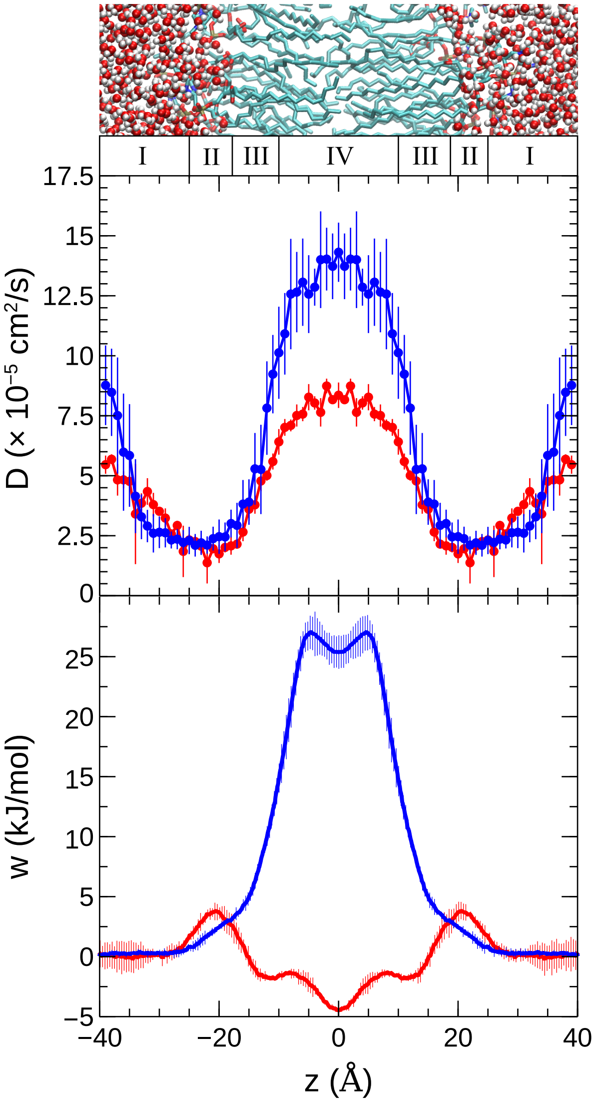

Figure 3: The diffusivity ($D(z)$, top) and potential of mean force ($w(z)$, bottom) of H_2O and O_2 permeating through a DPPC bilayer. The curves for H_2O are shown in blue while the curves for O_2 are shown in red. Simulations were performed at 323 K. The CHARMM36 lipid model and TIP3P water models were used. The PMF profiles were calculated from 20 ns H-REMD umbrella sampling simulations. The diffusivity profiles were calculated from the average of six 4 ns MD simulations using Eqn. 15.

this point in the membrane than it is in bulk solution, while a negative PMF indicates it is more soluble. A highly positive PMF inside the membrane results in a small permeability coefficient, consistent with a low probability of the solute partitioning inside the bilayer to this position.

Hydrophobic solutes like O_2 have a small increase in the PMF at the water-lipid interface. The PMF drops once the solute reaches the ester/tail regions (Regions III & IV). For many hydrophobic solutes, the PMF reaches a minimum at $z = 0$ Å, indicating that these hydrophobic compounds will concentrate at the center of the bilayer. The thermodynamic driving force for this effect was investigated by MacCallum et al. by decomposing the PMF of hexane permeation into enthalpy and entropy components (36). Although the PMF across the bilayer was broad and flat, with a minimum at the center, the entropy and enthalpy components of the PMF varied significantly as the solute moved across the bilayer. The enthalpy component disfavors partitioning of hexane at the center of the bilayer where it has weaker intermolecular interactions with the lower-density lipid tails, but this is counteracted by a more favorable entropy term because the solute has greater configurational freedom in the fluid-like bilayer center.

The PMF of water is typical for the permeation of a polar solute. The PMF of permeation for hydrophilic solutes do not show large changes in the headgroup or ester regions. These regions are easily accessible by the solvent, so the solutes are largely hydrated in these regions and can have stabilizing interactions with the head groups. The PMF increases abruptly when the solute enters the lipid chain region of the membrane (Region III). The PMF reaches a maximum in the lipid tail region (Region IV) that extends over

10 Å. The height of this barrier is closely correlated to the water/alkane partition coefficient of the solute. In the solubility-diffusion model, this high and broad barrier results in a small permeability coefficient, providing a rigorous theoretical basis for the Meyer–Overton rule.

Charged and hydrogen-bonding permeations show most distinct PMFs. These compounds remain partially hydrated by a finger of water molecules that extends from the headgroups into Regions III & IV. In permeation simulations of ionic compounds like Na^+, Cl^- (53), methylammonium (54), and methylguanidiniumlysine (55; 56), the solute remains hydrated by a cluster of water molecules even at the center of the bilayer. Sampling the PMF is particularly challenging because various hydration states must be sampled. Because of this variable hydration, the motion of the solute cannot be reliably described as Brownian motion of a single particle, so the solubility–diffusion model is not necessarily a valid means to calculate a permeability coefficient. Nevertheless, the PMF can still be interpretively useful.

4.1.3. Diffusivity Profiles

The diffusivity profiles of solutes follow some general trends. The diffusivity is high at the center of the membrane where the lipid tails are disordered and fluid-like. The diffusivity drops significantly in Region III, where the lipid tails are ordered and undergo slow rearrangements (57). The diffusivity remains at a depressed value in the headgroup/water interface region, but increases again when the solute enters solution (Region I). It should be noted that the diffusivity in the solution region will generally be overestimated by a factor of 2–3 when the TIP3P water model is used because this model has an erroneously low viscosity (58).

The diffusivity of larger permeants tends to be smaller than for smaller permeants. In Figure 3, the diffusivity of the diatomic O_2 is systematically smaller than for H_2O, which has only one non-hydrogen atom. This can be interpreted using the Stokes–Einstein equation (59),

$$D = \frac{k_B T}{6\pi\eta r} \tag{17}$$

which predicts that the diffusion coefficient of a solute in solution is inversely proportional to the molecular radius, r. The Stokes–Einstein diffusion coefficient also has an inverse dependence on the viscosity of the solvent (η), which would predict that solutes would diffuse more rapidly in low-friction regions of the bilayer.

Broadly speaking, the diffusivity of a solute varies by a factor of 5–6 across the bilayer. While this is a significant difference, the solubility-diffusion model permeability coefficient is only linearly dependent on the $D(z)$. As a result, the permeability of a solute is less sensitive to $D(z)$ than it is to $w(z)$, which has an exponential dependence. Furthermore, the high diffusivity in Region IV largely cancels the low diffusivity in Regions II & III. This generally supports the strategy of many researchers who have interpreted trends in permeability based only on the PMF; however, quantitative comparison to experimental permeability coefficients still require accurate calculations of the diffusivity profiles.

4.2. Applications of the Solubility-Diffusion Model

The 1994 paper by Marrink and Berdensen on the calculation of permeability coefficients from molecular simulation has been cited more than 500 times as of 2015. The model has been used to describe the permeation of solutes ranging from gases to nanoparticles. Table 2 summarizes 88 papers reporting analysis of membrane permeability using molecular simulation.

4.3. Effect of Cholesterol Content

One of the most significant contributions of the solubility–diffusion model has been in understanding the effect of cholesterol on membrane permeability. Cholesterol is a major component of eukaryotic cell membranes and has long been known to have strong effects on the membrane permeability of solutes. Generally, solutes permeate membranes with higher cholesterol content at lower rates (60; 61; 62).

One of the earliest studies was by Jedlovszky and Mezei (63) who estimated the PMF for permeation of 8 solutes (H_2O, O_2, CO, CO_2, NO, NH_3, $CHCl_3$, and formamide) through DMPC bilayers with varying cholesterol concentration and pointed to changes in the PMF as the cause of the reduced permeability. A later study by Hub et al. found that the PMF for the permeation of ammonia and carbon dioxide was increased when the cholesterol content of the membrane was high (64). The effect of cholesterol on the permeation of drug molecules has also been studied. Eriksson and Eriksson investigated the influence of cholesterol on the membrane permeability properties of the photodynamic drug, hypericin, and its mono- and tetra-brominated derivatives. The authors found that the calculated rate of permeation was lower at high cholesterol content due to higher PMF barriers.

Several simulation studies have examined the effect of bilayer cholesterol content on water permeation, which also decreases at high cholesterol content (65). Saito and Shinoda explored the effect of cholesterol content on the water-permeation PMFs of DPPC and PSM lipid bilayers. They found that with increasing cholesterol concentration, both DPPC and PSM lipid membranes displayed an increased PMF for water permeability; although the effect was more prominent in the PSM bilayers with 30 mol % of cholesterol content. Similarly, Issack and Peslherbe recently examined the influence of cholesterol on the PMF and diffusivity profiles for transmembrane water permeation. They found the PMF in Region III was significantly increased when the cholesterol content was high. A small decrease in diffusivity in Region IV had a secondary contribution.

One of the most comprehensive studies of the effect of cholesterol on permeation was reported by Wennberg et al. (27). The PMFs for solute permeation across 20 different lipid membranes containing one of four types of phospholipids (i.e., DMPC, DPPC, POPC, POPE) and cholesterol content that varied from 0 to 50 mol % were computed. The general trend from this study was that the PMFs for solute permeation were increased when the cholesterol content was high, particularly in Region 3, where the ring structure of cholesterol preferentially partitioned. Cholesterol is relatively rigid and packs tightly into the lipid tails, resulting in strong London dispersion interactions between the lipids and the cholesterol. A permeating solute disrupts these interactions and is generally unable to pack into the lipid tails as tightly as can cholesterol. As a result, the PMF for a solute permeating through Region III of a cholesterol-containing bilayer is increased, which decreases the rate of permeation. A subsequent study by Zocher et al. found the diffusivity of permeating solutes were generally independent of cholesterol content and changes in the PMF were the dominant effect on permeation rates (66).

5. Innovations in Modeling Permeation

5.1. Polarizable Models

Permeating solutes pass from the polar aqueous phase through the nonpolar membrane interior. In the course of permeation, the dielectric constant changes from $\epsilon = 78$ in bulk water to $\epsilon = 2$ in the lipid tail region. Polarizable solutes can experience a large induced polarization when dissolved in liquid water. This polarization effectively disappears when the solute moves to the nonpolar membrane interior. For solutes that can hydrogen-bond with water, this change in polarization is even more significant. Most simulations to date use fixed atomic charges to describe electrostatic interactions, so they are incapable of describing the effects of induced polarization.

Force fields that include the effects of induced polarization are gradually becoming available. A variety of polarizable models for biomolecules have been developed, including the Drude (67; 68), CHarge EQuilibration Method (CHEQ) (69), and the Atomic Multipole Optimized Energetics for Biomolecular Simulation (AMOEBA) models (70). Drude models are attractive for bilayer simulations because of their efficiency; polarizability is incorporated by tethering charged “Drude” particles to non-hydrogen atoms and propagating their positions dynamically (see Figure 4)

To date, only a handful of polarizable force fields for lipids are available. Lucas et al. reported a CHEQ polarizable model for DPPC lipids (71).. Separately, Robinson has developed a Drude model force field for cholesterol and sphingomyelin (72). Harder et al. developed a Drude polarizable model for DPPC to model the lipid monolayer-air interface (73). Chowdhary et al. refined this model to describe DPPC bilayers (74). It should be noted

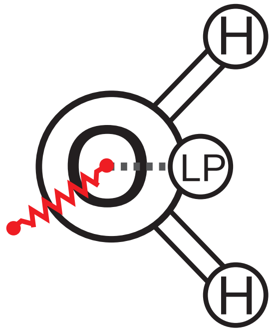

Figure 4: A schematic of the SWM4-NDP Drude polarize water molecule. Each water is comprised of three atomic centers (an oxygen and two hydrogens), a massless "lone-pair" particle is constrained to a position along the H–O–H bisector, and a negatively charged "Drude" particle that is tethered to the oxygen atom with a harmonic potential (red).

that this Drude DPPC model is actually less accurate in describing the lipid head group area and order parameters than the nonpolarizable CHARMM36 model, although this can likely be addressed by further refinement of the force field parameters.

A simulation of water permeation through a DMPC bilayer using a CHEQ model was reported by Bauer et al., who found the barrier in the PMF using various CHEQ polarizable models were in the 19–23 kJ/mol range, which were somewhat lower than the 26–30 kJ/mol barriers reported in other simulations (75). The permeability coefficient was not calculated in this study, so this result cannot be directly tested by comparison to the experimental value. There was a large change in polarization of the permeating water molecule; the dipole moment of water dropped from 2.6 D in bulk water to 1.88 D at the bilayer center.

Riahi and Rowley simulated the permeation of H_2O and H_2S through a

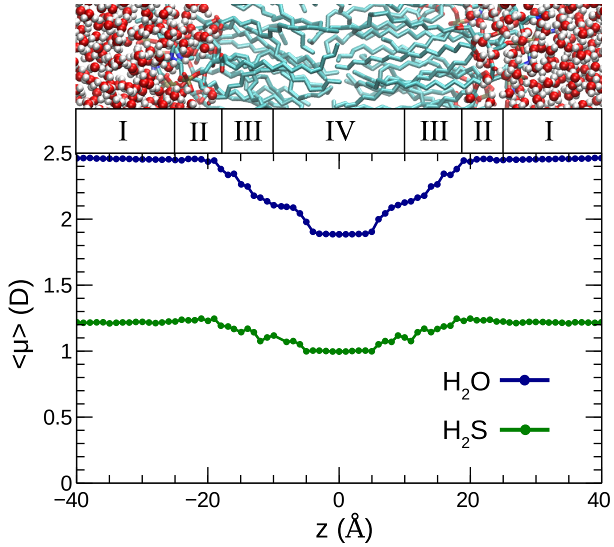

Figure 5: The dipole moments of H_2O (blue) and H_2S (green) solutes permeating across a DPPC bilayer. The average dipole of H_2O is high in solution ($\langle\mu\rangle = 2.5$ D) but drops to a value equal to its static permanent dipole ($\mu_0 = 1.8$ D) at the center of the bilayer. H_2S experiences a much smaller change ($\langle\mu\rangle = 1.2 \rightarrow 1.0$ D) The values are averaged from the umbrella sampling windows, calculated with a Drude polarizable model. Data from Ref. 28.

DPPC bilayer using the Drude polarizable model (28). The average dipole moment of H_2O decreased from 2.5 D to 1.9 D when it crossed into the center of the membrane interior, but the average dipole moment of H_2S only decreased from 1.2 D to 1.0 D. This is contrary to the trend in solute polarizability, as H_2S has a polarizability of 3.6 Å^3 while water has a polarizability of 1.45 Å^3 (Figure 5). Counterintuitively, molecules that are highly polarizable will not necessarily be strongly polarized in liquid water because high polarizability correlates to larger molecular radii. In the case of H_2S, the modest polarity and large radius of the sulfur atom precludes hydrogen bonding or other kinds of close-range polarizing interactions with water. Induced polarization is most significant in molecules that have a large static dipole moment and form hydrogen bonds with water molecules.

Although the rigorous inclusion of induced polarization is desirable conceptually, the results from simulations using polarizable models are not necessarily more accurate. For instance, the water-permeation PMF calculated using the Drude model is very similar to that calculated using many non-polarizable models. Non-polarizable force fields are often parameterized to reproduce the experimental solvation free energies of solutes. These energies correspond to the change in Gibbs energy when the solute is transferred from the gas phase to liquid water, which involves a similar change in solute polarization to what occurs during membrane permeation. These non-polarizable models will have the effect of induced polarization “baked in” through the parameterization, so the PMF barrier will be accurate. For example, the permanent dipole moments of molecules described with the non-polarizable GAFF model are systematically larger than the experimental gas phase values because of a systematic bias in the quantum chemical method used to assign the atomic charges (33; 76). In effect, this method of parameterization mimics the effect of induced polarization, although the physical basis for this is not entirely realistic. Likewise, the accuracy of a polarizable model is only as good as its parameterization.

Polarizable force fields can provide some other advantages for modeling permeation. Because of the larger parameter space and more physically realistic description of the system, they can be parameterized to describe a greater range of properties with greater accuracy. For instance, the SWM4-NDP Drude polarizable water model provides good descriptions of the dielectric constant and diffusion coefficients of water (77). Some popular nonpolarizable water models, like TIP3P, are significantly in error for the calculation of these properties. The water permeation rate calculated by Riahi and Rowley using the Drude model was in quantitative agreement with experiment, suggesting that the solubility-diffusion model combined with a Drude polarizable force field is an effective method for modeling permeation (28). Developing lipid models for use with more accurate non-polarizable water models, like TIP4P/2005 (78; 79), would address some of these limitations without requiring the use of polarizable models. Future development of both polarizable and nonpolarizable models for membrane permeation would benefit from being validated against the solvation energies and diffusion coefficients of the solutes in water and the liquid alkanes used to parameterize the lipid tails.

There are also several drawbacks associated with the use of polarizable force fields. The number of molecules that have been parameterized for simulations using polarizable force fields still lags behind established non-polarizable force fields. The computational cost of polarizable models is greater than non-polarizable force fields due to the need to calculate additional force field terms. Depending on the size and composition of the system, this can range from a factor of 2 for the Drude model to a factor of 20 for the AMOEBA model. Standard dual-Lagrangian implementations of the Drude model are also incompatible with replica exchange methods. As a result, the benefits of using a polarizable model must be weighed against increased statistical error because the configurational sampling is more limited.

Simulations of membrane permeation using polarizable models are now possible for select solutes and lipids. The development of polarizable models for additional solutes and lipids will extend this further in the coming years. These models will make it possible to quantitatively examine the role of polarization in membrane permeation and could allow a greater level of accuracy in cases where induced polarization is significant. The choice between a nonpolarizable or a polarizable model depends on the availability and accuracy of the force fields and whether sufficient sampling can be performed using the polarizable model.

5.2. Coarse Grain Models

Coarse grain models have also been used to simulate membrane permeation. These models reduce the computational expense of the simulation by using a simplified description of intermolecular interactions and grouping atoms into “bead” particles. The MARTINI model for lipids has been notably successful in describing many of the physical properties of bilayers (80; 81). Groups of atoms of a bilayer system are transformed into bead

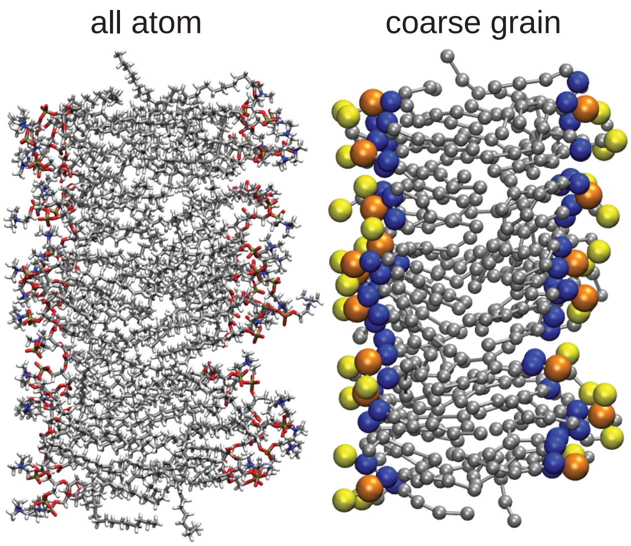

Figure 6: An all-atom POPC model bilayer (left) vs a MARTINI coarse grain model (right). Groups of 3–4 non-hydrogen atoms and the hydrogens bound to them are combined into a single "bead" particle in the coarse grain model.

particles. Each bead represents 3–4 non-hydrogen atoms of the lipid or solvent (Figure 6). The nonbonded interaction potentials of the various types of bead particles are parameterized to reproduce water-octanol partition coefficients. From this basic design, the surfactant properties of the bilayer arise intrinsically.

Through coarse-graining, much of the atomic-scale resolution of the system is lost. Despite this, the description of many bilayer physical and dynamic properties relevant to permeation is remarkably good. For example, the viscosity coefficient of MARTINI water is 7×10^{-4} Pa·s (at 323 K), in fairly good agreement with the experimental value of 5.5×10^{-4} Pa·s (82). The self-diffusion coefficients predicted by this model are more variable; the rate of diffusion of water and alkanes are in good agreement with experiment, but alcohols and lipids diffuse at rates up to 20 times faster than experiment (83). The water permeability of a MARTINI DPPC bilayer was estimated by direct simulation to be 1.5×10^{-3} cm/s, which is a reasonable value given the simplicity of the model (80).

Coarse grain models have been used to study many of the same solutes that have been studied using all atom models, including H_2O, gases, ions, and small organic molecules. Coarse grain models are particularly suitable for modeling permeation of nano-scale solutes that would be difficult to simulate at an appropriate scale with an atomistic model. These studies have included the permeation and partitioning of fullerenes and nanoparticles. These studies are summarized in Table 1.

For molecules that are too small to be coarse-grained without losing significant aspects of their chemical properties, multiscale models may be effective. Orsi and Essex developed a model where the permeant was described by an all-atom model but the solution and bilayer were coarse-grained (90). This model was generally effective at reproducing the permeability coefficients predicted by all-atom models.

Coarse grain models can be more computationally efficient than all atoms models by multiple orders of magnitude. Consequently, coarse grain simulations of permeation commonly include hundreds of lipids and simulations that are hundreds of nanoseconds long are routine. This is particularly significant when modeling large solutes that require large simulation cells and extensive sampling to calculate accurate $w(z)$ and $D(z)$ profiles. This advantage must be weighed against the loss of atomic detail in the model and quality of the coarse grained model used.

Table 1: Papers using coarse grained models to simulate membrane permeation.

Year	Ref.	Subject	Lipid
2007	84	effect of bilayer stretching on water permeation	DPPC
2008	85	permeation of fullerene	DPPC
2009	86	permeability of Xe, O_2, and CO_2	DCPC, DMPC, and DPPC
2009	46	permeability of acetamide, acetic acid, benzene, ethane, methanol, methylacetate, methylamine water	DMPC
2009	87	permeation of fullerene and fullerene derivatives	DPPC
2010	88	permeation of Na^+ and K^+	DPPC
2010	89	permeation of water	DPPC and MPPC
2010	90	pharmaceuticals (alprenolol, atenolol, and pindolol) and hormones (progesterone and testosterone)	DMPC
2012	91	Permeation of nanoparticle and nanoparticle with hydrophobic coating	DPPC
2012	92	Effect of nanoparticle size and velocity on membrane during permeation	DPPC
2013	93	nanoparticle with hydrophobic and hydrophilic coating	DPPC
2015	94	effect of surface functionalization of nanoparticles on permeation	DPPC

6. Conclusions

Molecular simulation has contributed significantly to the study of nonfacilitated membrane permeability. These simulations provide atomistic-scale insight into why solutes cross membranes at different rates and why the composition of the membrane affects permeability. The solubility-diffusion model has provided a method for the quantitative calculation of permeability coefficients from the potential of mean force and diffusivity profiles of the solutes on the transmembrane axis. Although accurate calculation of these profiles can be challenging, there are established computational strategies for computing them. More sophisticated molecular mechanical force fields will improve the accuracy of the underlying models. More representative configurational sampling through improvements in computing hardware and more efficient simulation algorithms will reduce statistical error. Coarse grain and polarizable force fields have promise in addressing the sampling issues and accuracy of permeation simulations, respectively. Once these issues are resolved, the quantitative accuracy of the underlying solubility-diffusion model can also be assessed.

There are many interesting subjects in nonfacilitated membrane permeation that remain unexplored. The success of molecular simulation in describing the effect of cholesterol content on permeability suggests that these techniques could be used to understand the effects of other aspects of membrane composition on permeability. Notably, most studies to date have used pure DPPC bilayers as a membrane model and simulations using mixed-lipid bilayers that are more representative of biological cell membranes have not been reported yet. Simulations may also be able to help resolve the controversy over purported exceptions to the Meyer–Overton rule (95; 96; 97; 98; 99).

Cell membranes are remarkable structures that emerge from the amphiphilic properties of the constituent lipids. The selective permeability of lipid bilayers is ultimately a simple phase partitioning effect that arises from complex intermolecular interactions. Appropriately, the solubility-diffusion model is a simple but effective theory for understanding the complex process of permeability. Marrink and Berendsen's 1994 paper that first demonstrated that permeability coefficients could be calculated quantitatively using molecular dynamics simulations has been cited over 500 times in the last 21 years and is undoubtedly a landmark paper in computational biophysics (22).

Acknowledgements

We thank NSERC of Canada for funding through the Discovery Grant program (Application 418505-2012). EAW thanks ACEnet and Memorial University for funding. Computational resources were provided by Compute Canada (RAPI: djk-615-ab) through the Calcul Quebec and ACEnet consortia. We thank Chris Neale for helpful comments.

References

[1] M. Edidin, Lipids on the frontier: a century of cell-membrane bilayers, Nature Reviews Molecular Cell Biology 4 (5) (2003) 414–418. doi:10.1038/nrm1102.

[2] G. van Meer, D. R. Voelker, G. W. Feigenson, Membrane lipids: where they are and how they behave, Nature Reviews Molecular Cell Biology 9 (2) (2008) 112–124. doi:10.1038/nrm2330.

[3] N. Ridgway, R. McLeod, Functional roles of lipids in membranes, in: Biochemistry of Lipids, Lipoproteins and Membranes, Elsevier Science, 2015, pp. 1–39.

[4] B. Hille, Ion Channels of Excitable Membranes (3rd Edition), 3rd Edition, Sinauer Associates Inc 2001-07, 2001.

[5] M. Luckey, Membrane Structural Biology: With Biochemical and Biophysical Foundations, Cambridge University Press, 2008.

[6] B. Roux, S. Bernèche, B. Egwolf, B. Lev, S. Y. Noskov, C. N. Rowley, H. Yu, Ion selectivity in channels and transporters, J. Gen. Physiol. 137 (5) (2011) 415–426. doi:10.1085/jgp.201010577.

[7] A. Volkov, S. Paula, D. Deamer, Two mechanisms of permeation of small neutral molecules and hydrated ions across phospholipid bilayers, Bioelectrochemistry and Bioenergetics 42 (2) (1997) 153–160, 13th International Symposium on Bioelectrochemistry and Bioenergetics. doi:http://dx.doi.org/10.1016/S0302-4598(96)05097-0.
URL `http://www.sciencedirect.com/science/article/pii/S0302459896050970`

[8] S. Mitragotri, M. E. Johnson, D. Blankschtein, R. Langer, An analysis of the size selectivity of solute partitioning, diffusion, and permeation across lipid bilayers, Biophysical Journal 77 (3) (1999) 1268–1283. doi:http://dx.doi.org/10.1016/S0006-3495(99)76978-X.

[9] A. Mälkiä, L. Murtomäki, A. Urtti, K. Kontturi, Drug permeation in biomembranes: In vitro and in silico prediction and influence of

physicochemical properties, Eur. J. Pharm. Sci. 23 (1) (2004) 13–47. doi:http://dx.doi.org/10.1016/j.ejps.2004.05.009.

[10] B. Faller, Artificial membrane assays to assess permeability, Curr. Drug Metab. 9 (2008) 886–892.

[11] H. Meyer, Zur theorie der alkoholnarkose, Archiv für experimentelle Pathologie und Pharmakologie 42 (2–4) (1899) 109–118. doi:10.1007/BF01834479.

[12] C. E. Overton, Studien über die Narkose; zugleich ein Beitrag zur allgemeinen Pharmakologie, Jena, Fischer, 1901.

[13] A. Walter, J. Gutknecht, Permeability of small nonelectrolytes through lipid bilayer membranes, The Journal of Membrane Biology 90 (3) (1986) 207–217. doi:10.1007/BF01870127.

[14] I. Bloch, A theory of membrane permeability: I, The bulletin of mathematical biophysics 6 (3) (1944) 85–92. doi:10.1007/BF02478238.

[15] H. Träuble, The movement of molecules across lipid membranes: A molecular theory, The Journal of Membrane Biology 4 (1) (1971) 193–208. doi:10.1007/BF02431971.

[16] A. Finkelstein, Water and nonelectrolyte permeability of lipid bilayer membranes, J. Gen. Physiol. 68 (1976) 127–135.

[17] J. L. MacCallum, D. P. Tieleman, Chapter 8 interactions between small molecules and lipid bilayers, in: S. E. Feller (Ed.),

Computational Modeling of Membrane Bilayers, Vol. 60 of Current Topics in Membranes, Academic Press, 2008, pp. 227 – 256. doi:http://dx.doi.org/10.1016/S1063-5823(08)00008-2.

[18] M. Orsi, J. W. Essex, Chapter 4 passive permeation across lipid bilayers: a literature review, in: Molecular Simulations and Biomembranes: From Biophysics to Function, The Royal Society of Chemistry, 2010, pp. 76–90. doi:10.1039/9781849732154-00076.

[19] D. G. Levitt, Interpretation of biological ion channel flux data–reaction-rate versus continuum theory, Annual Review of Biophysics and Biophysical Chemistry 15 (1) (1986) 29–57. doi:10.1146/annurev.bb.15.060186.000333.

[20] T. W. Allen, O. S. Andersen, B. Roux, Energetics of ion conduction through the gramicidin channel, Proceedings of the National Academy of Sciences 101 (1) (2004) 117–122. doi:10.1073/pnas.2635314100.

[21] J. M. Diamond, Y. Katz, Interpretation of nonelectrolyte partition coefficients between dimyristoyl lecithin and water, J. Membr. Biol. 17 (1) (1974) 121–154. doi:10.1007/BF01870176.

[22] S. J. Marrink, H. J. C. Berendsen, Simulation of water transport through a lipid membrane, J. Phys. Chem. 98 (1994) 4155–4168.

[23] H. J. C. Berendsen, S.-J. Marrink, Molecular dynamics of water transport through membranes: Water from solvent to solute, Pure Appl. Chem. 65 (1993) 2513–2520. doi:10.1351/pac199365122513.

[24] G. Parisio, M. Stocchero, A. Ferrarini, Passive membrane permeability: Beyond the standard solubility-diffusion model, J. Comp. Theory. Comput. 9 (12) (2013) 5236–5246. doi:10.1021/ct400690t.

[25] W. F. D. Bennett, D. P. Tieleman, The importance of membrane defects – lessons from simulations, Acc. Chem. Res. 47 (8) (2014) 2244–2251. doi:10.1021/ar4002729.

[26] C. Neale, C. Madill, S. Rauscher, R. Pomès, Accelerating convergence in molecular dynamics simulations of solutes in lipid membranes by conducting a random walk along the bilayer normal, J. Chem. Theory. Comput. 9 (8) (2013) 3686–3703. doi:10.1021/ct301005b.

[27] C. L. Wennberg, D. van der Spoel, J. S. Hub, Large influence of cholesterol on solute partitioning into lipid membranes, Journal of the American Chemical Society 134 (11) (2012) 53515361. doi:10.1021/ja211929h.

[28] S. Riahi, C. N. Rowley, Why can hydrogen sulfide permeate cell membranes?, J. Am. Chem. Soc. 136 (43) (2014) 15111–15113. doi:10.1021/ja508063s.

[29] W. L. Jorgensen, J. Chandrasekhar, J. D. Madura, R. W. Impey, M. L. Klein, Comparison of simple potential functions for simulating liquid water, The Journal of Chemical Physics 79 (2) (1983) 926–935. doi:10.1063/1.445869.

[30] W. L. Jorgensen, J. D. Madura, Temperature and size dependence for

monte carlo simulations of tip4p water, Molecular Physics 56 (6) (1985) 1381–1392. doi:10.1080/00268978500103111.

[31] O. Berger, O. Edholm, F. Jähnig, Molecular dynamics simulations of a fluid bilayer of dipalmitoylphosphatidylcholine at full hydration, constant pressure, and constant temperature, Biophys. J. 72 (5) (1997) 2002–2013. doi:http://dx.doi.org/10.1016/S0006-3495(97)78845-3.

[32] J. B. Klauda, R. M. Venable, J. A. Freites, J. W. O'Connor, D. J. Tobias, C. Mondragon-Ramirez, I. Vorobyov, A. D. MacKerell Jr., R. W. Pastor, Update of the CHARMM all-atom additive force field for lipids: validation on six lipid types, J. Phys. Chem. B 114 (2010) 7830–7843.

[33] J. Wang, R. M. Wolf, J. W. Caldwell, P. A. Kollman, D. A. Case, Development and testing of a general amber force field, J. Comput. Chem 25 (9) (2004) 1157–1174. doi:10.1002/jcc.20035.

[34] W. L. Jorgensen, J. Tirado-Rives, Potential energy functions for atomic-level simulations of water and organic and biomolecular systems, Proc. Natl. Acad. Sci. U.S.A. 102 (19) (2005) 6665–6670. arXiv:http://www.pnas.org/content/102/19/6665.full.pdf, doi:10.1073/pnas.0408037102.

[35] K. Vanommeslaeghe, E. Hatcher, C. Acharya, S. Kundu, S. Zhong, J. Shim, E. Darian, O. Guvench, P. Lopes, I. Vorobyov, A. D. Mackerell Jr., Charmm general force field: A force field for drug-like molecules compatible with the charmm all-atom additive biological force fields, J. Comput. Chem. 31 (4) (2010) 671–690. doi:10.1002/jcc.21367.

[36] J. L. MacCallum, D. P. Tieleman, Computer simulation of the distribution of hexane in a lipid bilayer: spatially resolved free energy, entropy, and enthalpy profiles, J. Am. Chem. Soc 128 (1) (2006) 125–130. doi:10.1021/ja0535099.

[37] C. Neale, C. Madill, S. Rauscher, R. Poms, Accelerating convergence in molecular dynamics simulations of solutes in lipid membranes by conducting a random walk along the bilayer normal, Journal of Chemical Theory and Computation 9 (8) (2013) 36863703. doi:10.1021/ct301005b.

[38] C. Neale, W. D. Bennett, D. P. Tieleman, R. Pomès, Statistical convergence of equilibrium properties in simulations of molecular solutes embedded in lipid bilayers, J. Chem. Theory Comput. 7 (2011) 4175–4188.

[39] Y. Sugita, A. Kitao, Y. Okamoto, Multidimensional replica-exchange method for free-energy calculations, The Journal of Chemical Physics 113 (15) (2000) 6042–6051. doi:http://dx.doi.org/10.1063/1.1308516.

[40] J. Kästner, Umbrella sampling, Wiley Interdisciplinary Reviews: Computational Molecular Science 1 (6) (2011) 932–942. doi:10.1002/wcms.66.

[41] S. Rauscher, C. Neale, R. Pomès, Simulated tempering distributed replica sampling, virtual replica exchange, and other generalized-ensemble methods for conformational sampling, J. Chem. Theory Comput. 5 (10) (2009) 2640–2662. doi:10.1021/ct900302n.

[42] K. Huang, A. E. García, Acceleration of lateral equilibration in mixed lipid bilayers using replica exchange with solute tempering, J. Chem. Theory Comput. 10 (10) (2014) 4264–4272. arXiv:http://dx.doi.org/10.1021/ct500305u, doi:10.1021/ct500305u.

[43] J. Comer, K. Schulten, C. Chipot, Diffusive models of membrane permeation with explicit orientational freedom, J. Chem. Theory Comput. 10 (2014) 2710–2718.

[44] G. Hummer, Position-dependent diffusion coefficients and free energies from bayesian analysis of equilibrium and replica molecular dynamics simulations, New J. Phys. 7 (2005) 34.

[45] R. Kubo, The fluctuation-dissipation theorem, Reports on Progress in Physics 29 (1) (1966) 255.

[46] M. Orsi, W. E. Sanderson, J. W. Essex, Permeability of small molecules through a lipid bilayer: A multiscale simulation study, J. Phys. Chem. B 113 (35) (2009) 12019–12029. doi:10.1021/jp903248s.

[47] T. B. Woolf, B. Roux, Molecular dynamics simulation of the gramicidin channel in a phospholipid bilayer, Proc. Natl. Acad. Sci. USA 91 (1994) 11631–11635.

[48] S. Crouzy, T. Woolf, B. Roux, A molecular dynamics study of gating in dioxolane-linked gramicidin a channels, Biophys. J. 67 (4) (1994) 1370–1386. doi:http://dx.doi.org/10.1016/S0006-3495(94)80618-6.

[49] M. F. Schumaker, R. Pomès, B. Roux, A combined molecular dynamics and diffusion model of single proton conduc-

tion through gramicidin, Biophys. J. 79 (6) (2000) 2840–2857. doi:http://dx.doi.org/10.1016/S0006-3495(00)76522-2.

[50] M. Allen, D. Tildesley, Computer Simulation of Liquids, Oxford Science Publications, Clarendon Press, Oxford, 1989.

[51] M. L. Mugnai, R. Elber, Extracting the diffusion tensor from molecular dynamics simulation with milestoning, J. Chem. Phys 142 (1) (2015) 014105. doi:http://dx.doi.org/10.1063/1.4904882.

[52] J. Comer, C. Chipot, F. D. Gonzlez-Nilo, Calculating position-dependent diffusivity in biased molecular dynamics simulations, Journal of Chemical Theory and Computation 9 (2) (2013) 876–882. doi:10.1021/ct300867e.

[53] I. V. Khavrutskii, A. A. Gorfe, B. Lu, J. A. McCammon, Free energy for the permeation of na + and cl ions and their ion-pair through a zwitterionic dimyristoyl phosphatidylcholine lipid bilayer by umbrella integration with harmonic fourier beads, Journal of the American Chemical Society 131 (5) (2009) 17061716. doi:10.1021/ja8081704.

[54] L. Li, I. Vorobyov, T. W. Allen, The different interactions of lysine and arginine side chains with lipid membranes, The Journal of Physical Chemistry B 117 (40) (2013) 11906–11920. doi:10.1021/jp405418y.

[55] J. L. MacCallum, W. D. Bennett, D. P. Tieleman, Transfer of arginine into lipid bilayers is nonadditive, Biophys. J. 101 (1) (2011) 110–117. doi:http://dx.doi.org/10.1016/j.bpj.2011.05.038.

[56] D. Sun, J. Forsman, C. E. Woodward, Evaluating force fields for the computational prediction of ionized arginine and lysine side-chains partitioning into lipid bilayers and octanol, Journal of Chemical Theory and Computation 11 (4) (2015) 1775–1791. doi:10.1021/ct501063a.

[57] D. Bemporad, J. Essex, C. Luttmann, Permeation of small molecules through a lipid bilayer: A computer simulation study, J. Phys. Chem. B 108 (2004) 4875–4884.

[58] Y. Mao, Y. Zhang, Thermal conductivity, shear viscosity and specific heat of rigid water models, Chemical Physics Letters 542 (2012) 37–41. doi:10.1016/j.cplett.2012.05.044.

[59] A. Einstein, Investigations on the Theory of the Brownian Movement, Dover Books on Physics Series, Dover Publications, 1956.

[60] D. Papahadjopoulos, M. Cowden, H. Kimelberg, Role of cholesterol in membranes effects on phospholipid-protein interactions, membrane permeability and enzymatic activity, Biochimica et Biophysica Acta (BBA) - Biomembranes 330 (1) (1973) 8–26. doi:10.1016/0005-2736(73)90280-0.

[61] L. R. D. Young, K. A. Dill, Solute partitioning into lipid bilayer membranes, Biochemistry 27 (14) (1988) 5281–5289. arXiv:http://dx.doi.org/10.1021/bi00414a050, doi:10.1021/bi00414a050.

[62] E. C. Yan, K. B. Eisenthal, Effect of cholesterol on molecular transport of organic cations across liposome bilayers probed by

second harmonic generation, Biophys. J. 79 (2) (2000) 898–903. doi:http://dx.doi.org/10.1016/S0006-3495(00)76345-4.

[63] P. Jedlovszky, M. Mezei, Effect of cholesterol on the properties of phospholipid membranes. 2. free energy profile of small molecules, J. Phys. Chem. B 107 (22) (2003) 53225332. doi:10.1021/jp021951x.

[64] J. S. Hub, F. K. Winkler, M. Merrick, B. L. de Groot, Potentials of mean force and permeabilities for carbon dioxide, ammonia, and water flux across a rhesus protein channel and lipid membranes, Journal of the American Chemical Society 132 (38) (2010) 1325113263. doi:10.1021/ja102133x.

[65] J. C. Mathai, S. Tristram-Nagle, J. F. Nagle, M. L. Zeidel, Structural determinants of water permeability through the lipid membrane, The Journal of General Physiology 131 (1) (2008) 69–76. doi:10.1085/jgp.200709848.

[66] F. Zocher, D. van der Spoel, P. Pohl, J. Hub, Local partition coefficients govern solute permeability of cholesterol-containing membranes, Biophysical Journal 105 (12) (2013) 27602770. doi:10.1016/j.bpj.2013.11.003.

[67] G. Lamoureux, B. Roux, Modeling induced polarization with classical drude oscillators: Theory and molecular dynamics simulation algorithm, J. Chem. Phys. 119 (6) (2003) 3025–3039. doi:10.1063/1.1589749.

[68] P. Lopes, B. Roux, A. MacKerell Jr., Molecular modeling and dynamics studies with explicit inclusion of electronic polarizability: theory and applications, Theor. Chem. Acc. 124 (2009) 11–28.

[69] S. Patel, C. L. Brooks III, Fluctuating charge force fields: recent developments and applications from small molecules to macromolecular biological systems, Molecular Simulation 32 (3-4) (2006) 231–249. doi:10.1080/08927020600726708.

[70] J. W. Ponder, C. Wu, P. Ren, V. S. Pande, J. D. Chodera, M. J. Schnieders, I. Haque, D. L. Mobley, D. S. Lambrecht, J. Robert A. DiStasio, M. Head-Gordon, G. N. I. Clark, M. E. Johnson, T. Head-Gordon, Current status of the AMOEBA polarizable force field, The Journal of Physical Chemistry B 114 (8) (2010) 2549–2564. arXiv:http://dx.doi.org/10.1021/jp910674d, doi:10.1021/jp910674d.

[71] J. E. Davis, S. Patel, Charge equilibration force fields for lipid environments: Applications to fully hydrated DPPC bilayers and DMPC-embedded gramicidin A, J. Phys. Chem. B 113 (27) (2009) 9183–9196. doi:10.1021/jp901088g.

[72] D. Robinson, A polarizable force-field for cholesterol and sphingomyelin, J. Chem. Theory Comput. 9 (5) (2013) 2498–2503. doi:10.1021/ct400103e.

[73] E. Harder, A. D. MacKerell, Jr., B. Roux, Many-body polarization effects and the membrane dipole potential, J. Am. Chem. Soc. 131 (8) (2009) 2760–2761. doi:10.1021/ja806825g.

[74] J. Chowdhary, E. Harder, P. E. M. Lopes, L. Huang, A. D. MacKerell, Jr., B. Roux, A polarizable force field of dipalmitoylphosphatidylcholine based on the classical drude model for molecular dynamics simulations of lipids, J. Phys. Chem. B 117 (31) (2013) 9142–9160. doi:10.1021/jp402860e.

[75] B. A. Bauer, T. R. Lucas, D. J. Meninger, S. Patel, Water permeation through DMPC lipid bilayers using polarizable charge equilibration force fields, Chem. Phys. Lett. 508 (4-6) (2011) 289–294. doi:10.1016/j.cplett.2011.04.052.

[76] A. L. Hickey, C. N. Rowley, Benchmarking quantum chemical methods for the calculation of molecular dipole moments and polarizabilities, J. Chem. Phys. A 118 (20) (2014) 3678–3687. doi:10.1021/jp502475e.

[77] G. Lamoureux, E. Harder, I. V. Vorobyov, B. Roux, A. D. MacKerell Jr., A polarizable model of water for molecular dynamics simulations of biomolecules, Chem. Phys. Lett. 418 (13) (2006) 245–249. doi:10.1016/j.cplett.2005.10.135.

[78] J. L. F. Abascal, C. Vega, A general purpose model for the condensed phases of water: TIP4P/2005, J. Chem. Phys. 123 (23) (2005) 234505. doi:http://dx.doi.org/10.1063/1.2121687.

[79] D. Rozmanov, P. G. Kusalik, Transport coefficients of the TIP4P-2005 water model, J. Chem. Phys 136 (4) (2012) 044507. doi:http://dx.doi.org/10.1063/1.3677196.

[80] S. J. Marrink, A. H. de Vries, A. E. Mark, Coarse grained model for semiquantitative lipid simulations, J. Phys. Chem. B 108 (2) (2004) 750–760. arXiv:http://dx.doi.org/10.1021/jp036508g, doi:10.1021/jp036508g.

[81] S. J. Marrink, D. P. Tieleman, Perspective on the martini model, Chem. Soc. Rev. 42 (2013) 6801–6822. doi:10.1039/C3CS60093A.

[82] W. den Otter, S. Shkulipa, Intermonolayer friction and surface shear viscosity of lipid bilayer membranes, Biophys. J. 93 (2) (2007) 423–433. doi:http://dx.doi.org/10.1529/biophysj.107.105395.

[83] D. H. de Jong, A molecular view on the organizational complexity of proteins in membranes, Ph.D. thesis, University of Groningen (2013).

[84] A. Gauthier, B. Joós, Stretching effects on the permeability of water molecules across a lipid bilayer, J. Chem. Phys. 127 (10) (2007) –. doi:http://dx.doi.org/10.1063/1.2764079.

[85] J. Wong-Ekkabut, S. Baoukina, W. Triampo, I.-M. Tang, D. P. Tieleman, L. Monticelli, Computer simulation study of fullerene translocation through lipid membranes, Nat. Nanotechnol. 3 (6) (2008) 363–368. doi:10.1038/nnano.2008.130.

[86] H. Yuan, C. J. Jameson, S. Murad, Exploring gas permeability of lipid membranes using coarse-grained molecular dynamics, Molecular Simulation 35 (10-11) (2009) 953–961. doi:10.1080/08927020902763839.

[87] R. S. G. D'Rozario, C. L. Wee, E. J. Wallace, M. S. P. Sansom, The

interaction of c60 and its derivatives with a lipid bilayer via molecular dynamics simulations, Nanotechnology 20 (11) (2009) 115102.

[88] S. O. Yesylevskyy, L. V. Schäfer, D. Sengupta, S. J. Marrink, Polarizable water model for the coarse-grained martini force field, PLoS Comput Biol 6 (6) (2010) e1000810. doi:10.1371/journal.pcbi.1000810.

[89] N. D. Winter, G. C. Schatz, Coarse-grained molecular dynamics study of permeability enhancement in DPPC bilayers by incorporation of lysolipid, J. Phys. Chem B 114 (15) (2010) 5053–5060. doi:10.1021/jp911309s.

[90] M. Orsi, J. Michel, J. W. Essex, Coarse-grain modelling of DMPC and DOPC lipid bilayers, Journal of Physics: Condensed Matter 22 (15) (2010) 155106.

[91] B. Song, H. Yuan, C. J. Jameson, S. Murad, Role of surface ligands in nanoparticle permeation through a model membrane: a coarse-grained molecular dynamics simulations study, Mol. Phys. 110 (18) (2012) 2181–2195. doi:10.1080/00268976.2012.668964.

[92] B. Song, H. Yuan, S. V. Pham, C. J. Jameson, S. Murad, Nanoparticle permeation induces water penetration, ion transport, and lipid flip-flop, Langmuir 28 (49) (2012) 16989–17000. doi:10.1021/la302879r.

[93] P. Gkeka, L. Sarkisov, P. Angelikopoulos, Homogeneous hydrophobichydrophilic surface patterns enhance permeation of nanoparticles through lipid membranes, The Journal of Physical Chemistry Letters 4 (11) (2013) 1907–1912. doi:10.1021/jz400679z.

[94] P. A. Oroskar, C. J. Jameson, S. Murad, Surface-functionalized nanoparticle permeation triggers lipid displacement and water and ion leakage, Langmuir 31 (3) (2015) 1074–1085. doi:10.1021/la503934c.

[95] A. V. Thomae, H. Wunderli-Allenspach, S. D. Krmer, Permeation of aromatic carboxylic acids across lipid bilayers: The ph-partition hypothesis revisited, Biophysical Journal 89 (3) (2005) 1802–1811. doi:http://dx.doi.org/10.1529/biophysj.105.060871.

[96] S. M. Saparov, Y. N. Antonenko, P. Pohl, A new model of weak acid permeation through membranes revisited: Does overton still rule?, Biophysical Journal 90 (11) (2006) L86 – L88. doi:http://dx.doi.org/10.1529/biophysj.106.084343.

[97] J. M. A. Grime, M. A. Edwards, N. C. Rudd, P. R. Unwin, Quantitative visualization of passive transport across bilayer lipid membranes, Proc. Natl. Acad. Sci. U.S.A. 105 (38) (2008) 14277–14282. arXiv:http://www.pnas.org/content/105/38/14277.full.pdf, doi:10.1073/pnas.0803720105.

[98] A. Missner, P. Kügler, Y. N. Antonenko, P. Pohl, Passive transport across bilayer lipid membranes: Overton continues to rule, Proc. Natl. Acad. Sci. U.S.A. 105 (52) (2008) E123. arXiv:http://www.pnas.org/content/105/52/E123.full.pdf, doi:10.1073/pnas.0809606106.

[99] A. Missner, P. Pohl, 110 years of the meyeroverton rule: Predicting membrane permeability of gases and other small

compounds, ChemPhysChem 10 (9-10) (2009) 1405–1414. doi:10.1002/cphc.200900270.

[100] S. J. Marrink, H. J. C. Berendsen, Permeation process of small molecules across lipid membranes studied by molecular dynamics simulations, J. Phys. Chem 100 (41) (1996) 16729–16738. doi:10.1021/jp952956f.

[101] M. A. Wilson, A. Pohorille, Mechanism of unassisted ion transport across membrane bilayers, Journal of the American Chemical Society 118 (28) (1996) 65806587. doi:10.1021/ja9540381.

[102] K. Tu, M. Tarek, M. L. Klein, D. Scharf, Effects of anesthetics on the structure of a phospholipid bilayer: Molecular dynamics investigation of halothane in the hydrated liquid crystal phase of dipalmitoylphosphatidylcholine, Biophysical Journal 75 (5) (1998) 21232134. doi:10.1016/s0006-3495(98)77655-6.

[103] P. Jedlovszky, M. Mezei, Calculation of the free energy profile of H_2O, O_2, CO, CO_2, NO, and $CHCl_3$ in a lipid bilayer with a cavity insertion variant of the widom method, Journal of the American Chemical Society 122 (21) (2000) 51255131. doi:10.1021/ja000156z.

[104] J. A. Söderhäll, A. Laaksonen, Molecular dynamics simulations of ubiquinone inside a lipid bilayer, J. Phys. Chem. B 105 (38) (2001) 93089315. doi:10.1021/jp011001w.

[105] D. Bas, D. Dorison-Duval, S. Moreau, P. Bruneau, C. Chipot, Rational determination of transfer free energies of small drugs across the wa-

teroil interface, Journal of Medicinal Chemistry 45 (1) (2002) 151159. doi:10.1021/jm010289a.

[106] J. Ulander, A. Haymet, Permeation across hydrated DPPC lipid bilayers: Simulation of the titrable amphiphilic drug valproic acid, Biophysical Journal 85 (6) (2003) 34753484. doi:10.1016/s0006-3495(03)74768-7.

[107] B. G. Dzikovski, V. A. Livshits, D. Marsh, Oxygen permeation profile in lipid membranes: Comparison with transmembrane polarity profile, Biophysical Journal 85 (2) (2003) 10051012. doi:10.1016/s0006-3495(03)74539-1.

[108] D. Bemporad, J. W. Essex, C. Luttmann, Permeation of small molecules through a lipid bilayer: a computer simulation study, J. Phys. Chem. B 108 (15) (2004) 4875–4884. doi:10.1021/jp035260s.

[109] J. Milhaud, New insights into water–phospholipid model membrane interactions, Biochimica et Biophysica Acta (BBA) - Biomembranes 1663 (1-2) (2004) 1951. doi:10.1016/j.bbamem.2004.02.003.

[110] W. Shinoda, M. Mikami, T. Baba, M. Hato, Molecular dynamics study on the effects of chain branching on the physical properties of lipid bilayers: 2. permeability, J. Phys. Chem B 108 (26) (2004) 9346–9356. arXiv:http://dx.doi.org/10.1021/jp035998+, doi:10.1021/jp035998+.

[111] P. Mukhopadhyay, H. J. Vogel, D. P. Tieleman, Distribution of pentachlorophenol in phospholipid bilayers: A molecular dynamics

study, Biophysical Journal 86 (1) (2004) 337345. doi:10.1016/s0006-3495(04)74109-0.

[112] K. Shinoda, W. Shinoda, T. Baba, M. Mikami, Comparative molecular dynamics study of ether- and ester-linked phospholipid bilayers, J. Chem. Phys. 121 (19) (2004) 9648. doi:10.1063/1.1806791.

[113] B. Hoff, E. Strandberg, A. S. Ulrich, D. P. Tieleman, C. Posten, 2h-NMR study and molecular dynamics simulation of the location, alignment, and mobility of pyrene in POPC bilayers, Biophysical Journal 88 (3) (2005) 1818–1827. doi:10.1529/biophysj.104.052399.

[114] D. Bemporad, C. Luttmann, J. Essex, Behaviour of small solutes and large drugs in a lipid bilayer from computer simulations, Biochimica et Biophysica Acta (BBA) - Biomembranes 1718 (1-2) (2005) 1–21. doi:10.1016/j.bbamem.2005.07.009.

[115] T. Sugii, S. Takagi, Y. Matsumoto, A molecular-dynamics study of lipid bilayers: Effects of the hydrocarbon chain length on permeability, J. Chem. Phys. 123 (18) (2005) 184714. doi:10.1063/1.2102900.

[116] P. Matsson, C. A. S. Bergström, N. Nagahara, S. Tavelin, U. Norinder, P. Artursson, Exploring the role of different drug transport routes in permeability screening, Journal of Medicinal Chemistry 48 (2) (2005) 604613. doi:10.1021/jm049711o.

[117] J. L. MacCallum, D. P. Tieleman, Computer simulation of the distribution of hexane in a lipid bilayer: spatially resolved free energy, en-

tropy, and enthalpy profiles, Journal of the American Chemical Society 128 (1) (2006) 125130. doi:10.1021/ja0535099.

[118] K. E. Norman, H. Nymeyer, Indole localization in lipid membranes revealed by molecular simulation, Biophysical Journal 91 (6) (2006) 20462054. doi:10.1529/biophysj.105.080275.

[119] J. C. Mathai, S. Tristram-Nagle, J. F. Nagle, M. L. Zeidel, Structural determinants of water permeability through the lipid membrane, The Journal of General Physiology 131 (1) (2007) 6976. doi:10.1085/jgp.200709848.

[120] J. L. MacCallum, W. F. D. Bennett, D. P. Tieleman, Distribution of amino acids in a lipid bilayer from computer simulations, Biophysical Journal 94 (9) (2008) 33933404. doi:10.1529/biophysj.107.112805.

[121] J. F. Nagle, J. C. Mathai, M. L. Zeidel, S. Tristram-Nagle, Theory of passive permeability through lipid bilayers, The Journal of General Physiology 131 (1) (2007) 7785. doi:10.1085/jgp.200709849.

[122] E. R. McCarney, B. D. Armstrong, R. Kausik, S. Han, Dynamic nuclear polarization enhanced nuclear magnetic resonance and electron spin resonance studies of hydration and local water dynamics in micelle and vesicle assemblies, Langmuir 24 (18) (2008) 1006210072. doi:10.1021/la800334k.

[123] E. Erdtman, D. J. dos Santos, L. Lögren, L. A. Eriksson, Modelling the behavior of 5-aminolevulinic acid and its alkyl esters in

a lipid bilayer, Chemical Physics Letters 463 (1-3) (2008) 178182. doi:10.1016/j.cplett.2008.08.021.

[124] K. Shinoda, W. Shinoda, M. Mikami, Efficient free energy calculation of water across lipid membranes, Journal of Computational Chemistry 29 (12) (2008) 19121918. doi:10.1002/jcc.20956.

[125] Y. Wang, Y. Z. Ohkubo, E. Tajkhorshid, Chapter 12 gas conduction of lipid bilayers and membrane channels, Computational Modeling of Membrane Bilayers (2008) 343367doi:10.1016/s1063-5823(08)00012-4.

[126] P.-L. Chau, K.-M. Tu, K. Liang, S. Chan, N. Matubayasi, Free-energy change of inserting halothane into different depths of a hydrated dmpc bilayer, Chemical Physics Letters 462 (1-3) (2008) 112115. doi:10.1016/j.cplett.2008.07.037.

[127] J. E. Davis, O. Rahaman, S. Patel, Molecular dynamics simulations of a dmpc bilayer using nonadditive interaction models, Biophysical Journal 96 (2) (2009) 385402. doi:10.1016/j.bpj.2008.09.048.

[128] C. Wei, A. Pohorille, Permeation of membranes by ribose and its diastereomers, Journal of the American Chemical Society 131 (29) (2009) 1023710245. doi:10.1021/ja902531k.

[129] C. Das, P. D. Olmsted, M. G. Noro, Water permeation through stratum corneum lipid bilayers from atomistic simulations, Soft Matter 5 (22) (2009) 4549. doi:10.1039/b911257j.

[130] T. J. Müller, F. Müller-Plathe, A comparison of sulfur mustard and heptane penetrating a dipalmitoylphosphatidylcholine bilayer

membrane, Journal of Hazardous Materials 168 (1) (2009) 13–24. doi:10.1016/j.jhazmat.2009.01.140.

[131] A. A. Mamonov, V. E. Stefanov, B. F. Shchegolev, Molecular dynamics investigation of nitric oxide (ii) interaction with a model biological membrane, Biochemistry (Moscow) Supplement Series A: Membrane and Cell Biology 3 (2) (2009) 231238. doi:10.1134/s1990747809020172.

[132] L. Monticelli, E. Salonen, P. C. Ke, I. Vattulainen, Effects of carbon nanoparticles on lipid membranes: a molecular simulation perspective, Soft Matter 5 (22) (2009) 4433. doi:10.1039/b912310e.

[133] M. Orsi, J. W. Essex, Permeability of drugs and hormones through a lipid bilayer: insights from dual-resolution molecular dynamics, Soft Matter 6 (16) (2010) 3797. doi:10.1039/c0sm00136h.

[134] M. B. Boggara, R. Krishnamoorti, Partitioning of nonsteroidal antiinflammatory drugs in lipid membranes: A molecular dynamics simulation study, Biophysical Journal 98 (4) (2010) 586595. doi:10.1016/j.bpj.2009.10.046.

[135] S. L. Fiedler, A. Violi, Simulation of nanoparticle permeation through a lipid membrane, Biophysical Journal 99 (1) (2010) 144152. doi:10.1016/j.bpj.2010.03.039.

[136] S. Mitragotri, Y. G. Anissimov, A. L. Bunge, H. F. Frasch, R. H. Guy, J. Hadgraft, G. B. Kasting, M. E. Lane, M. S. Roberts, Mathematical models of skin permeability: An overview,

International Journal of Pharmaceutics 418 (1) (2011) 115129. doi:10.1016/j.ijpharm.2011.02.023.

[137] R. C. Van Lehn, A. Alexander-Katz, Penetration of lipid bilayers by nanoparticles with environmentally-responsive surfaces: simulations and theory, Soft Matter 7 (24) (2011) 11392. doi:10.1039/c1sm06405c.

[138] H. Saito, W. Shinoda, Cholesterol effect on water permeability through DPPC and PSM lipid bilayers: A molecular dynamics study, J. Phys. Chem. B 115 (51) (2011) 1524115250. doi:10.1021/jp201611p.

[139] E. S. E. Eriksson, L. A. Eriksson, The influence of cholesterol on the properties and permeability of hypericin derivatives in lipid membranes, Journal of Chemical Theory and Computation 7 (3) (2011) 560574. doi:10.1021/ct100528u.

[140] B. A. Bauer, T. R. Lucas, D. J. Meninger, S. Patel, Water permeation through dmpc lipid bilayers using polarizable charge equilibration force fields, Chemical Physics Letters 508 (4-6) (2011) 289294. doi:10.1016/j.cplett.2011.04.052.

[141] C. Wei, A. Pohorille, Permeation of nucleosides through lipid bilayers, J. Phys. Chem. B 115 (13) (2011) 36813688. doi:10.1021/jp112104r.

[142] M. Minozzi, G. Lattanzi, R. Benz, M. P. Costi, A. Venturelli, P. Carloni, Permeation through the cell membrane of a boron-based β-lactamase inhibitor, PLoS ONE 6 (8) (2011) e23187. doi:10.1371/journal.pone.0023187.

[143] M. Paloncov, K. Berka, M. Otyepka, Convergence of free energy profile of coumarin in lipid bilayer, Journal of Chemical Theory and Computation 8 (4) (2012) 12001211. doi:10.1021/ct2009208.

[144] A. E. Cardenas, G. S. Jas, K. Y. DeLeon, W. A. Hegefeld, K. Kuczera, R. Elber, Unassisted transport of n -acetyl- l -tryptophanamide through membrane: Experiment and simulation of kinetics, J. Phys. Chem. B 116 (9) (2012) 27392750. doi:10.1021/jp2102447.

[145] Z. Ghaemi, M. Minozzi, P. Carloni, A. Laio, A novel approach to the investigation of passive molecular permeation through lipid bilayers from atomistic simulations, J. Phys. Chem. B 116 (29) (2012) 87148721. doi:10.1021/jp301083h.

[146] M. B. Boggara, M. Mihailescu, R. Krishnamoorti, Structural association of nonsteroidal anti-inflammatory drugs with lipid membranes, Journal of the American Chemical Society 134 (48) (2012) 1966919676. doi:10.1021/ja3064342.

[147] J. Lin, B. Novak, D. Moldovan, Molecular dynamics simulation study of the effect of dmso on structural and permeation properties of dmpc lipid bilayers, J. Phys. Chem. B 116 (4) (2012) 12991308. doi:10.1021/jp208145b.

[148] K. Fujimoto, N. Yoshii, S. Okazaki, Free energy profiles for penetration of methane and water molecules into spherical sodium dodecyl sulfate micelles obtained using the thermodynamic integration method com-

bined with molecular dynamics calculations, J. Chem. Phys. 136 (1) (2012) 014511. doi:10.1063/1.3671997.

[149] M. Darvas, P. N. M. Hoang, S. Picaud, M. Sega, P. Jedlovszky, Anesthetic molecules embedded in a lipid membrane: a computer simulation study, Physical Chemistry Chemical Physics 14 (37) (2012) 12956. doi:10.1039/c2cp41581j.

[150] B. W. Holland, C. G. Gray, B. Tomberli, Calculating diffusion and permeability coefficients with the oscillating forward-reverse method, Phys. Rev. E 86 (3). doi:10.1103/physreve.86.036707.

[151] R. Notman, J. Anwar, Breaching the skin barrier insights from molecular simulation of model membranes, Advanced Drug Delivery Reviews 65 (2) (2013) 237250. doi:10.1016/j.addr.2012.02.011.

[152] M. Paloncov, K. Berka, M. Otyepka, Molecular insight into affinities of drugs and their metabolites to lipid bilayers, J. Phys. Chem. B 117 (8) (2013) 24032410. doi:10.1021/jp311802x.

[153] D. I. Kopelevich, One-dimensional potential of mean force underestimates activation barrier for transport across flexible lipid membranes, J. Chem. Phys. 139 (13) (2013) 134906. doi:10.1063/1.4823500.

[154] P. Gkeka, L. Sarkisov, P. Angelikopoulos, Homogeneous hydrophobichydrophilic surface patterns enhance permeation of nanoparticles through lipid membranes, The Journal of Physical Chemistry Letters 4 (11) (2013) 19071912. doi:10.1021/jz400679z.

[155] R. V. Swift, R. E. Amaro, Back to the future: Can physical models of passive membrane permeability help reduce drug candidate attrition and move us beyond QSPR?, Chemical Biology and Drug Design 81 (1) (2012) 6171. doi:10.1111/cbdd.12074.

[156] A. E. Cardenas, R. Elber, Computational study of peptide permeation through membrane: searching for hidden slow variables, Molecular Physics 111 (22-23) (2013) 35653578. doi:10.1080/00268976.2013.842010.

[157] P. Podlouck, K. Berka, G. Fabre, M. Paloncov, J.-L. Duroux, M. Otyepka, P. Trouillas, Lipid bilayer membrane affinity rationalizes inhibition of lipid peroxidation by a natural lignan antioxidant, J. Phys. Chem. B 117 (17) (2013) 50435049. doi:10.1021/jp3127829.

[158] J. M. Nitsche, G. B. Kasting, Permeability of fluid-phase phospholipid bilayers: Assessment and useful correlations for permeability screening and other applications, J. Pharm. Sci. 102 (6) (2013) 20052032. doi:10.1002/jps.23471.

[159] N. A. Krylov, V. M. Pentkovsky, R. G. Efremov, Nontrivial behavior of water in the vicinity and inside lipid bilayers as probed by molecular dynamics simulations, ACS Nano 7 (10) (2013) 94289442. doi:10.1021/nn4042392.

[160] B. C. G. Karlsson, G. D. Olsson, R. Friedman, A. M. Rosengren, H. Henschel, I. A. Nicholls, How warfarins structural diversity influ-

ences its phospholipid bilayer membrane permeation, J. Phys. Chem. B 117 (8) (2013) 23842395. doi:10.1021/jp400264x.

[161] B. Qiao, M. Olvera de la Cruz, Driving force for water permeation across lipid membranes, The Journal of Physical Chemistry Letters 4 (19) (2013) 32333237. doi:10.1021/jz401730s.

[162] T. H. F. Thake, J. R. Webb, A. Nash, J. Z. Rappoport, R. Notman, Permeation of polystyrene nanoparticles across model lipid bilayer membranes, Soft Matter 9 (43) (2013) 10265. doi:10.1039/c3sm51225h.

[163] M. Kang, S. M. Loverde, Molecular simulation of the concentration-dependent interaction of hydrophobic drugs with model cellular membranes, J. Phys. Chem. B 118 (41) (2014) 1196511972. doi:10.1021/jp5047613.

[164] F.-Y. Bian, J.-W. Zhang, D. Wang, S.-C. Xu, Molecular dynamics simulation of the permeation of methyldopa through POPC phospholipid bilayer membrane, Acta Physico-Chimica Sinica 30 (10) (2014) 1947–1956. doi:10.3866/PKU.WHXB201408271.

[165] G. H. Peters, M. Werge, M. N. Elf-Lind, J. J. Madsen, G. F. Velardez, P. Westh, Interaction of neurotransmitters with a phospholipid bilayer: A molecular dynamics study, Chemistry and Physics of Lipids 184 (2014) 717. doi:10.1016/j.chemphyslip.2014.08.003.

[166] J. Comer, K. Schulten, C. Chipot, Diffusive models of membrane permeation with explicit orientational freedom, Journal of Chemical Theory and Computation 10 (7) (2014) 27102718. doi:10.1021/ct500209j.

[167] R. M. Cordeiro, Reactive oxygen species at phospholipid bilayers: Distribution, mobility and permeation, Biochimica et Biophysica Acta (BBA) - Biomembranes 1838 (1) (2014) 438444. doi:10.1016/j.bbamem.2013.09.016.

[168] A. Khajeh, H. Modarress, The influence of cholesterol on interactions and dynamics of ibuprofen in a lipid bilayer, Biochimica et Biophysica Acta (BBA) - Biomembranes 1838 (10) (2014) 24312438. doi:10.1016/j.bbamem.2014.05.029.

[169] B. W. Holland, M. D. Berry, C. G. Gray, B. Tomberli, A permeability study of O_2 and the trace amine p-tyramine through model phosphatidylcholine bilayers, PLoS ONE 10 (6) (2015) e0122468. doi:10.1371/journal.pone.0122468.

[170] A. E. Cardenas, R. Shrestha, L. J. Webb, R. Elber, Membrane permeation of a peptide: It is better to be positive, J. Phys. Chem. B 119 (21) (2015) 64126420. doi:10.1021/acs.jpcb.5b02122.

[171] S. Jalili, M. Saeedi, Study of curcumin behavior in two different lipid bilayer models of liposomal curcumin using molecular dynamics simulation, Journal of Biomolecular Structure and Dynamics (2015) 114doi:10.1080/07391102.2015.1030692.

[172] B. B. Issack, G. H. Peslherbe, Effects of cholesterol on the thermodynamics and kinetics of passive transport of water through lipid membranes, J. Phys. Chem. B 119 (29) (2015) 93919400. doi:10.1021/jp510497r.

[173] L. Yang, J. T. Kindt, Simulation study of the permeability of a model lipid membrane at the fluidsolid phase transition, Langmuir 31 (7) (2015) 21872195. doi:10.1021/la504269t.

[174] R. Thind, D. W. O'Neill, A. Del Regno, R. Notman, Ethanol induces the formation of water-permeable defects in model bilayers of skin lipids, Chem. Commun. 51 (25) (2015) 54065409. doi:10.1039/c4cc08527b.

[175] M. Casalegno, G. Raos, G. Sello, Hydrophobic aggregation and collective absorption of dioxin into lipid membranes: insights from atomistic simulations, Phys. Chem. Chem. Phys. 17 (4) (2015) 23442348. doi:10.1039/c4cp05466k.

Table 2: Papers using molecular simulation to model nonfacillitated membrane permeation

Year	Ref.	Subject	Lipid
1994	22	permeation of H_2O	DPPC
1996	100	permeation of O_2, NH_3, and Lennard-Jones spheres	DPPC
1996	101	permeation of Na^+ and Cl^-	GMO
1998	102	effects of halothane on lipid bilayer structure	DPPC
2000	103	permeability of H_2O, O_2, CO, CO_2, NO, $CHCl_3$	DMPC
2001	104	permeation of ubiquinone	DPPC
2002	105	permeability of organic molecules (antipyrine, caffeine, ganciclovir, α-D-glucose)	dodecane chains
2003	106	permeation of valproic acid	DPPC
2003	63	effect of cholesterol on the permeability of small molecules (H_2O, O_2, CO, CO_2, NO, NH_3, $CHCl_3$, and CH_3NO)	DMPC
2003	107	permeation of oxygen	DMPC
2004	108	permeation of small organic molecules	DPPC
2004	109	interactions of water molecules with lipid membranes	PCs/PEs

2004	108	permeation of small organic molecules (acetamide, acetic acid, benzene, ethane, methanol, methyl acetate, methylamine, water)	DPPC
2004	108	permeation of small molecules (acetamide, acetic acid, benzene, ethane, methanol, methyl acetate, methylamine, water)	DPPC
2004	110	effects of chain branching on water and neutral solute permeability	DPPC/DPhPC
2004	111	permeation and effects of pentachlorophenol (PCP)	POPE/POPC
2004	112	effects of ether- and ester-linked lipid bilayers on solute (H_2O and O_2) permeability	ether-DPhPC/ester-DPhPC
2005	113	permeation and interaction of pyrene	POPC
2005	114	permeation of small solutes (acetic acid, benzene, ethane, methanol, methyl acetate, methylamine, water) and large drugs (alprenolol, atenolol, pindolol)	DPPC
2005	115	effects of lipid hydrocarbon chain length on oxygen, water and nitic oxide permeability	DLPC/DMPC/DPPC

2005	116	influence of different drug transport routes	Caco-2, 2/4/A1, hexadecane membrane models
2006	117	permeation of hexane	DOPC
2006	118	localization and orientation of indole and benzene	POPC
2007	119	permeation of water	POPC/ DOPC/ DMPC/ DLPC/ diC22:1PC/ DOPS/ DLPE
2008	85	permeation of fullerene and effects on membrane properties	DOPC/ DPPC
2008	120	permeation of amino acids	DOPC
2008	121	permeability of water	POPC / DOPC / DMPC / DLPC / diC22:1PC

2008	122	permeation of water	8-carbon alkyl-phenol poly-oxyethylene/oleate
2008	123	permeability and behavioral effects of 5-aminolevulunic acid and its ester derivatives	DPPC
2008	124	permeation of water	DPhPC
2008	125	permeation of O_2 and CO_2	POPE
2008	126	effects of halothane as a function of pressure in different membrane depths	DMPC
2009	53	permeation of Na^+ and Cl^-	DMPC
2009	127	permeability of water	DMPC
2009	128	permeation of ribose, aribinose and xylose	POPC
2009	129	permeation of water	CER2 bilayer
2009	130	permeation of sulfur mustard and heptane	DPPC
2009	131	permeation of NO	PC/PE
2009	132	effects of carbon nanoparticles on lipid membranes	DPPC/DMPC
2010	133	permeation of drugs (alprenolol, atenolol, pindolol) and hormones (progesterone, testosterone)	DMPC

2010	134	permeation of aspirin and ibuprofen	DPPC
2010	135	permeation of buckyball-sized nanoparticles	DMPC
2010	64	permeation of NH_3 and CO_2	POPE/ 3:1 POPE:POPG/ 1:1 POPE:POPC/ POPC
2011	136	predictive modeling of skin permeation	ceramide class of lipids
2011	137	permeation of nanoparticles with mixed hydrophobic/ hydrophilic surface functionalization	hydrophilic/ hydrophobic beads
2011	138	effect of cholesterol on water permeability	DPPC/ PSM
2011	139	Infuence of cholesterol on the permeability of hypericin and its brominated derivatives	DPPC
2011	133	permeation of triclocarbon and triclosan	DOPC
2011	140	permeation of water	DMPC
2011	141	permeation of nucleosides	POPC
2011	142	permeation of benzo[b]-thiophene-2-boronic acid (BZB)	POPC

2012	27	effect of cholesterol on partitioning of ethanol, ammonia, nitric oxide, propane, benzene, and pentane	POPE/ POPC/ DMPC/ DPPC
2012	143	partitioning of couramin	DOPC
2012	144	permeation of tryptophan	DOPC
2012	145	permeation of ethanol molecules	POPC
2012	146	permeation and structural influence of ibubrofen	DOPC
2012	147	effect of DMSO on water permeability	DMPC
2012	148	permeation of methane and water molecules	SDS micelles
2012	149	effect of anesthetic molecules on lipid membrane properties	DPPC
2012	150	permeation of water	DPPC
2013	151	permeation and chemical approaches of molecules in breaching skin lipid barrier	ceramide skin lipid
2013	37	permeation of n-propylguanidinium	POPC
2013	152	permeability of cytochrome P450 substrates (caffeine, chlorzaxazone, couramin, ibuprofen, debrisoquine) and metabolites (paraxanthine, 6-hydroxychlorzoxazone, 7-hydroxycoumarin, 3-hydroxyibuprofen, 4-hydroxydebrisoquine)	DOPC/ POPG
2013	153	permeation of fullerene-like nanoparticles	DPPC

2013	154	permeation of nanoparticles with hydrophobic-hydrophilic surface patterns	DPPC
2013	155	permeability prediction of candidate drug compounds	DMPC
2013	156	permeation of N-acetyl-L-tryptophanamide (NATA)	DOPC
2013	157	permeation of argenteane and 3,3'-dimethoxy-1,1'-biphenyl-2,2'-diol	DOPC/PLPC
2013	158	permeability analysis of selected molecules	egg lecithin/DMPC
2013	159	permeation of water	DOPC/ DPPC/ DOPS/ 9:1 DOPC:DPPC/ 3:1 POPG:POPE
2013	160	permeation and structural diversity of warfarin	DOPC
2013	161	permeation of water	DPPC/ DLPS
2013	66	effect of cholesterol on solute (NH_3, pyridine, TEA, NO) permeability	DOPE/ DOPC/ PLE
2013	162	permeation of polystyrene nanoparticles	DPPC
2014	28	permeation of H_2S and H_2O	DPPC

2014	163	interaction and permeation properties of paclitaxel	POPC
2014	164	permeation of methyldopa	POPC
2014	165	interactions and permeation properties of neurotransmitters (GABA, GLY, ACH, GLU)	DPPC
2014	166	permeation of water/ethanol	POPC
2014	167	permeability of reactive oxygen species (O_2, singlet oxygen, O_2^-, H_2O_2, HO, HO_2)	POPC
2014	168	influence of cholesterol on ibuprofen permeation	DMPC
2015	169	permeation of O_2 and p-tyramine	DPPC/ PC bilayers
2015	170	permeation of tryptophan molecule	DOPC
2015	171	permeation and effect of circumin in lipid bilayers	DMPG/ DPPC
2015	172	effect of cholesterol on water permeability	DPPC
2015	173	effect of lipid phase composition on particle permeation	model system (a group of neutral five-site molecules)

2015	174	effect of ethanol on water transport properties of CER2 bilayers	CER2
2015	175	permeation of dioxin	DPPC

DPPC: 1,2-dipalmitoyl-sn-glycero-3-phosphocholine, POPC: 1-palmitoyl-2-oleoyl-sn-glycero-3-phosphocholine, DMPC: 1,2-dimyristoyl-d54-sn-glycero-3-phosphocholine, CER2: N-lignoceroyl-D-erythro-sphingosine, DOPC: 1,2-dioleoyl-sn-glycero-3-phosphocholine, POPE: 1-palmitoyl-2-oleoyl-sn-glycero-3-phosphoethanolamine, DLPC: 1,2-didodecanoyl-sn-glycero-3-phosphocholine, DMPG: 1,2-dimyristoyl-sn-glycero-3-phospho-(1'-rac-glycerol), DLPS: 1,2-dilauroyl-sn-glycero-3-phospho-L-serine, POPG: 1-palmitoyl-2-oleoyl-sn-glycero-3-phospho-(1'-rac-glycerol)